

Resilient Edge Service Placement and Workload Allocation under Uncertainty

Jiaming Cheng, *Student Member, IEEE*, Duong Tung Nguyen, *Member, IEEE*,
and Vijay K. Bhargava, *Life Fellow, IEEE*

Abstract—In this paper, we study an optimal service placement and workload allocation problem for a service provider (SP), who can procure resources from numerous edge nodes to serve its users. The SP aims to improve the user experience while minimizing its cost, considering various system uncertainties. To tackle this challenging problem, we propose a novel resilience-aware edge service placement and workload allocation model that jointly captures the uncertainties of resource demand and node failures. The first-stage decisions include the optimal service placement and resource procurement, while the optimal workload allocation is determined in the second stage after the uncertainties are disclosed. The salient feature of the proposed model is that it produces a placement and procurement solution that is robust against any possible realization of the uncertainties. By leveraging the column-and-constraint generation method, we introduce two iterative algorithms that can converge to an exact optimal solution within a finite number of iterations. We further suggest an affine decision rule approximation approach for solving large-scale problem instances in a reasonable time. Extensive numerical results are shown to demonstrate the advantages of the proposed model and solutions.

Index Terms—Resilient edge computing, failure resilience, adaptive robust optimization, service placement, workload allocation, demand uncertainty, edge node failure, reliability, edge computing market, decision-making under uncertainty.



1 INTRODUCTION

Cloud computing has played an essential role in dealing with the ever-growing data traffic over the past decade. However, along with the proliferation of mobile devices and services, new applications such as augmented/virtual reality (AR/VR), autonomous driving, manufacturing automation, real-time analytics, and tactile Internet have imposed more stringent requirements on the communication network. Since cloud data centers (DC) are often located far away from end-users and data sources, it requires a wholesale rethinking of the network architecture to economically meet these requirements. To this end, edge computing (EC) has emerged as a vital technology that augments the cloud to mitigate network traffic, improve user experience, and enable novel Internet of Things (IoT) applications.

Fig. 1 illustrates the new network architecture where an EC layer lies between the cloud and the end-devices. Indeed, edge nodes (ENs) can reside anywhere along the edge-to-cloud continuum [1]. An EN may consist of one or multiple edge servers. Also, an EN can be co-located with a point of aggregation (POA). The user requests and sensor data are typically aggregated at POAs (e.g., switches/routers, base stations) before being transmitted to ENs or the cloud for further processing, analysis, and storage. By distributing cloud resources closer to the users, things, and sensors, EC offers significant advantages and capabilities, such as local data processing and analytics, distributed caching, and

enhanced security. Also, EC enables the implementation of various low-latency and high-reliability applications.

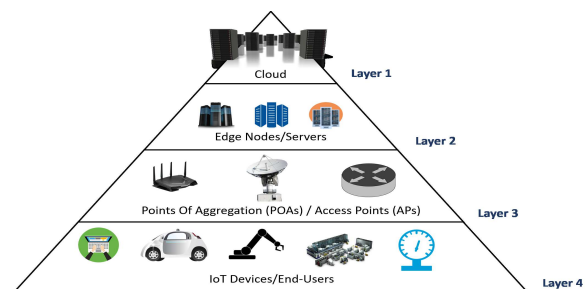


Fig. 1: Edge network architecture

Despite tremendous potential, EC is still in its early days and many open problems remained to be addressed. In this work, we focus on the optimal service placement and workload allocation problem for a delay-sensitive service (e.g., AR/VR, real-time translation, remote robotics, cloud gaming). To enhance the user experience, the service provider (SP) can provision the service onto different distributed ENs to reduce the delay between the users and computing nodes. The SP serves a large number of users located in different areas. The main objective of the SP is to maximize the service quality while minimizing the total operating cost.

Due to the heterogeneity of the ENs, it is challenging to select suitable nodes for service placement. Specifically, while placing the service on more ENs can lower the overall delay, it also increases the SP's cost. Furthermore, unlike the traditional cloud with a limited number of large cloud DCs, there are numerous geographically distributed heterogeneous ENs with different sizes and configurations. In addition, resource prices at different ENs can vary significantly. Therefore, some ENs closer to the users may not

Jiaming Cheng and Vijay K. Bhargava are with the Department of Electrical and Computer Engineering, University of British Columbia, Vancouver, BC, Canada. Email: {jiaming, vijayb}@ece.ubc.ca.

Duong Tung Nguyen is with the Ira A. Fulton Schools of Engineering, Arizona State University, Tempe, AZ, United States. Email: duongnt@asu.edu. This research was supported, in part, by the Natural Sciences and Engineering Research Council of Canada. (Corresponding author: Duong Tung Nguyen).

be selected due to their higher prices [2]. Besides service placement, the SP also has to determine the amount of resource to purchase from each selected EN. The service placement and resource procurement decisions are often referred to as service provisioning, which is constrained by the operating budget of the SP.

Given the provisioning decisions, the SP will optimally allocate the workloads from different areas to the ENs, which have installed the service, to minimize the overall network delay. If all system parameters are known exactly, the joint service placement and workload allocation problem can be formulated as a deterministic mixed-integer linear program (MILP), which can be solved efficiently using off-the-shelf MILP solvers. In practice, many system parameters are uncertain. Thus, the SP normally uses the forecast values of these parameters as input to the MILP. However, this deterministic approach can be inefficient if the actual values significantly different from the forecast values. For instance, if the actual demand is noticeably higher than the forecast demand, under-provisioning may occur frequently, which results in dropping requests and increasing unmet demand. On the other hand, if the actual demand is lower than the forecast demand, over-provisioning happens, which unnecessarily increases the operating cost of the SP.

In addition to demand uncertainty, the unpredictability of EN failures can notoriously affect the system performance. An EN can fully or partially fail due to various reasons (e.g., extreme weather events, natural disasters, malware, cyber-attacks, software malfunctions, power outage, links/routers/switches/servers at the EN fail). If the provisioning solution of the SP contains an EN that fails during the operation period, the demand initially assigned to that EN has to be reallocated to the other selected ENs. Thus, EN failures can deteriorate the user experience since user requests may be reassigned to ENs that are distant from them. Furthermore, if the procured resources at the other ENs are insufficient to meet the reallocated demand, a portion of the workload will be dropped, which is undesirable.

How to ensure an edge system works properly and automatically adapts and optimizes its operation during extreme events is an important and challenging question. Addressing this question can help build up a resilient EC system. In this work, we propose a novel resilience-aware two-stage robust model for an SP, who provides a delay-sensitive service. The proposed model can assist the SP to compute an optimal resource provisioning solution that can hedge against the uncertainties of edge resource demand and EN failures.

While stochastic optimization (SO) is a popular tool for decision-making under uncertainty, it usually requires to know the probability distribution of uncertain data, which is hard to obtain. Moreover, the uncertainty realization during the operation period may not follow the historical pattern [2]. Additionally, in SO, it is difficult to properly model discrete uncertainties such as EN failure events. Thus, we advocate robust optimization (RO) [3] to tackle the joint service placement and workload allocation problem. In RO, the uncertainties are captured by parametric sets, known as uncertainty sets, which are much easier to derive than exact probability distributions. Also, the EN failures can be modeled intuitively using cardinality constrained sets [9].

In our studied problem, the resource provisioning deci-

sion needs to be made before the actual workload allocation. Thus, instead of using the traditional static RO approach that makes all decisions at the same time and can be quite conservative, we employ the two-stage adaptive robust optimization (ARO) approach [2], [4], [5] to address the problem. To the best of our knowledge, this is the first two-stage robust model for the resilient edge service placement and workload allocation problem. This work is significantly different from our previous work [2] in several aspects. First, [2] considers only demand uncertainty while this work jointly considers the uncertainties of both demand and node failures. Second, a weighting factor is introduced to express the attitude of the SP towards the risk of uncertainties. Third, we do not consider the cloud option in this work since the service is delay-sensitive. Finally, we propose two new efficient solutions for solving the formulated problem. Our main contributions are summarized as follows:

- *Modeling*: We propose a novel resilience-aware two-stage robust model for joint optimization of edge service placement, resource procurement, and workload allocation. The uncertainties of demand and EN failures are explicitly integrated into the proposed model which consists of the service placement and resource procurement in the first stage as well as the workload allocation decision in the second stage.
- *Solution Approaches*: First, based on the column and constraint generation (CCG) method [4], we develop an iterative algorithm to solve the problem in a master-subproblem framework. Second, unlike [4] that uses the Karush–Kuhn–Tucker (KKT) conditions to solve the subproblem, we propose to solve the subproblem using linear programming (LP) duality when the demand uncertainty budget is integer. Third, since the running-time of CCG-based algorithms is sensitive to the uncertainty sets, we introduce an affine decision rule approximation approach, which is independent of the set sizes, to solve large-scale problem instances. Our proposed solutions are novel in the context of cloud and edge computing.
- *Simulation*: Extensive numerical results are shown to demonstrate the superior performance of the proposed ARO model compared to benchmark models. We also illustrate the benefits of considering both the demand and failure uncertainties. Finally, sensitivity analyses are conducted to examine the impacts of important system parameters on the optimal solution.

The rest of the paper is organized as follows. In Section 2, we present the system model and problem formulation. The solution approaches are introduced in Section 3, followed by the numerical results in Section 4. Section 5 discuss related work. Finally, the conclusions are given in Section 6.

2 SYSTEM MODEL AND PROBLEM FORMULATION

2.1 System Model

In this paper, we examine the edge resource procurement and management for an SP, who provides a delay-sensitive service (e.g., AR/VR, cloud gaming). While the SP does not own any EN, it can buy edge resources from an EC market, which consists of numerous geographically distributed heterogeneous ENs. The SP has subscribers located in different

areas, where user requests in each area are aggregated at an AP. To reduce the network delay and enhance the user experience, the SP can place the service onto the ENs to serve its users directly at the edge. Hence, two major concerns for the SP are where to install its service and how much computing resource to buy from each EN. Given the procured edge resources, the SP will decide how to optimally assign workloads from different APs to the ENs. Fig. 2 depicts the system model with five areas and four ENs. The service is installed on EN1, EN2, and EN4. When there is no failures, user requests in area 4 and area 5 can be served by EN4 (i.e., their closest EN). However, when EN4 fails, the workload from these areas can be reassigned to another EN (e.g., EN2) that has installed the service.

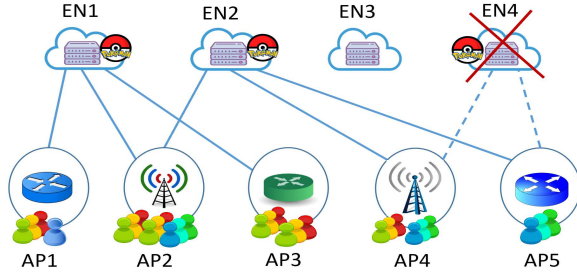


Fig. 2: System model

The SP is assumed to be a price-taker and has a budget B for purchasing edge resources for usage during the scheduling period (e.g., an hour, a day). Let i be the area index and \mathcal{I} be the set of areas, each of which is represented by an AP. The resource demand in area i is λ_i . Define j and \mathcal{J} as the EN index and the set of ENs, respectively. The resource capacity of EN j is C_j . Also, p_j is the price of one unit of computing resource at EN j . The delay between AP i and EN j is $d_{i,j}$. In practice, an EN may need to satisfy certain hardware and software requirements to operate the service. For instance, the service can be only deployed on ENs that support Pytorch and Ubuntu. Additionally, for a delay-sensitive service, the requests in an area should be served by ENs that are not too far from that area (e.g., the network delay should not exceed a certain delay threshold). Hence, we use a binary indicator $a_{i,j}$ to indicate whether EN j can serve demand from area i or not. Specifically, $a_{i,j} = 1$ if the demand from area i can be handled by EN j .

In the first stage, the SP optimizes the service placement and resource procurement decisions. The placement decision at EN j is represented by a binary variable t_j which equals to 1 if the service is installed at the EN. The amount of resource purchased from EN j is denoted by y_j . Define $t = (t_1, t_2, \dots, t_J)$ and $y = (y_1, y_2, \dots, y_J)$. In the first stage, the SP also optimizes the workload allocation decision $x_{i,j}$ based on the forecast demand λ_i^f . Given the first-stage decisions y and t , in the second stage, the SP optimally reallocates the actual demand to different ENs, which have installed the service in the first stage, under the worst-case uncertainty realization. Since the exact demand and EN failures are not known to the SP in the first stage, the procured resources may not be sufficient to serve the actual demand. Hence, a portion of the user requests may be dropped. Denote by q_i and P_i the amount of unmet demand and the penalty for each unit of unmet demand in area i ,

respectively. Also, let $w_{i,j}$ be the workload allocated from area i to EN j in the second stage. We often refer to q_i and $w_{i,j}$ as the recourse actions.

Depending on specific market settings, the SP may or may not be allowed to adjust the amount of purchased resource during the actual operation period. In our model, we do not allow the SP to adjust y_j in the second stage, which follows the current practice where cloud providers often require the buyers to purchase resources for usage for a minimum amount of time (e.g., one hour, one day) [2], [30]. Also, during the operation period, the demand can fluctuate significantly. Thus, the EN owners may not want the SP to frequently adjust y_j for short intervals because the economic benefit is small while the management cost increases. Our model can be easily extended to allow the SP to readjust the amount of resource in the second stage.

TABLE 1: NOTATIONS

| Notation | Meaning |
|------------------|--|
| EN, AP | Edge Node, Access Point |
| \mathcal{I}, I | Set and number of areas (APs) |
| \mathcal{J}, J | Set and number of ENs |
| i, j | Area (AP) index and EN index |
| C_j | Resource capacity of EN j |
| p_j | Unit price of computing resource at EN j |
| f_j | Service placement cost at EN j |
| $a_{i,j}$ | $\{0, 1\}$, "1" if EN j can serve demand from area i |
| $d_{i,j}$ | Delay between AP i and EN j |
| B | Budget of the SP |
| β | Delay penalty parameter |
| P_i | Penalty parameter for unmet demand in area i |
| ρ | Weighting factor between costs in two stages |
| λ_i^f | Forecast demand in area i |
| s_j | Storage cost at EN j |
| $x_{i,j}$ | Resource demand from area i served by EN j |
| $w_{i,j}$ | Workload from area i to EN j in the second stage |
| y_j | Amount of resource procurement at EN j |
| q_i | Amount of unmet demand in area i |
| t_j | $\{0, 1\}$, "1" if the service is installed at EN j |
| l_j^0 | $\{0, 1\}$, "1" if the service is initially available at EN j |
| z_j | $\{0, 1\}$, "1" if EN j fails |
| λ_i | Actual demand in area i |
| K | Node failure budget |
| Γ | Demand uncertainty budget |
| \mathcal{Z} | Node failure uncertainty set |
| \mathcal{D} | Demand uncertainty set |

2.2 Uncertainty Modeling

Since the exact demand and node failures are usually cannot be predicted accurately at the time of making the first-stage decisions, these system uncertainties need to be properly captured and integrated into the decision-making model of the SP. In RO, uncertain parameters are modeled by uncertainty sets, which represent an infinite number of scenarios. The uncertainty sets are usually constructed to balance between the robustness and conservativeness of the robust solution and to make the underlying optimization problem computationally tractable [3]. Similar to our previous work [2], we employ a polyhedral uncertainty set, which is widely-used in the RO literature [3]–[6], to model the demand uncertainty. Define $\lambda = (\lambda_1, \lambda_2, \dots, \lambda_I)$ and $\bar{\lambda} = (\bar{\lambda}_1, \bar{\lambda}_2, \dots, \bar{\lambda}_I)$ as the vector of the actual demands and the vector of the nominal values of the demands in different areas. Note that I is the number of areas (i.e., $I = |\mathcal{I}|$). Also, let $\bar{\lambda}_i$ be the maximum deviation of the demand in area

i from the nominal value $\bar{\lambda}_i$. Define $\tilde{\lambda} = (\tilde{\lambda}_1, \tilde{\lambda}_2, \dots, \tilde{\lambda}_I)$ as the vector of maximum demand deviations. Then, the actual demand λ_i belongs to the range of $[\bar{\lambda}_i, \bar{\lambda}_i + \tilde{\lambda}_i]$. This range is normally inferred from the forecast value of the demand. The forecast demand λ_i^f in area i is $\bar{\lambda}_i + \frac{\tilde{\lambda}_i}{2}$. The polyhedral demand uncertainty set \mathcal{D} can be expressed as follows:

$$\mathcal{D} = \left\{ \lambda : \lambda_i = \bar{\lambda}_i + g_i \tilde{\lambda}_i; g_i \in [0, 1], \forall i; \sum_i g_i \leq \Gamma \right\}, \quad (1)$$

where Γ is called the demand uncertainty budget, which controls the conservative level of the robust solution [2]–[6]. The uncertainty budget is set by the SP and can take any value between 0 and I . The demand uncertainty set enlarges as Γ increases. If $\Gamma = I$, \mathcal{D} becomes a box uncertainty set.

Besides the demand uncertainty, the SP also faces unpredictable failures of ENs during the operation period. To capture the uncertainty of the failure situation in the edge network, we employ a cardinality constrained uncertainty set, which is commonly-used to describe discrete uncertainties [9]. Let z_j be a binary indicator which equals to 1 if EN j fails. The failure uncertainty set \mathcal{Z} can be represented as:

$$\mathcal{Z} = \left\{ z_j \in \{0, 1\}^{|\mathcal{J}|} : \sum_j z_j \leq K \right\}, \quad (2)$$

where the integer K expresses the maximum number of ENs that can fail at the same time. In other words, the proposed solution is robust against up to K simultaneous EN failures. Obviously, $K \leq |\mathcal{J}| = J$. As K increases, the optimal solution becomes more robust. However, it is also more conservative (i.e., higher resource provisioning cost). If K is set to be zero, it implies that the SP does not consider potential node failures in its decision-making process. The SP can choose suitable values of Γ and K to control the level of robustness of the optimal solution. We use the following set Ξ to jointly capture the uncertainties of demand and EN failures.

$$\Xi = \left\{ (\lambda, \mathbf{z}) \in \mathbb{R}_+^{|\mathcal{I}|} \times \mathbb{B}^{|\mathcal{J}|} : \lambda \in \mathcal{D}, z \in \mathcal{Z} \right\}. \quad (3)$$

2.3 Problem Formulation

We are now ready to describe the two-stage robust model which assists the SP to minimize its cost while enhancing the user experience. The first-stage decision variables include the service placement (t), resource procurement (y), and the workload allocation (x). In the second stage, the SP optimizes the actual workload allocation (w) and the amount of unmet demand (q) under the worst-case realization of the uncertainties. These two stages are coupled by the service placement and resource procurement variables.

The SP aims to minimize the weighted sum of its operating cost, delay cost, and penalty cost for unmet demand. The operating cost consists of the service placement cost and edge resource procurement cost. If the SP decides to place the service onto EN j that does not have the service installed at the beginning of the scheduling period, the service needs to be downloaded from the cloud or a nearby EN, then be installed at the EN. In this case, it incurs a cost f_j for installing the service onto EN j . Clearly, if the service is available at EN j at the beginning, this cost becomes zero. Let l_j^0 be a binary indicator which is equal to 1 if the service

is initially available at EN j . The total service placement cost C^p over all the ENs can be expressed as follows.

$$C^p = \sum_j f_j (1 - l_j^0) t_j. \quad (4)$$

If the SP places the service at EN j , it needs to pay a storage cost that depends on the size of the service and the length of the scheduling period. Let s_j be the storage cost for the service at EN j . Then, the total storage cost C^s is:

$$C^s = \sum_j s_j t_j. \quad (5)$$

The computing resource cost at EN j equals to the amount of procured resource y_j multiplied by the resource price p_j . Thus, the total computing resource cost C^c is:

$$C^c = \sum_j p_j y_j. \quad (6)$$

The delay cost between area i and EN j is proportional to the amount of workload allocation from area i to EN j and the network delay between them. Thus, the total delay costs $C^{d,1}$ and $C^{d,2}$ in the first stage and the second stage, respectively, are:

$$C^{d,1} = \beta \sum_{i,j} d_{i,j} x_{i,j}; \quad C^{d,2} = \beta \sum_{i,j} d_{i,j} w_{i,j}. \quad (7)$$

Finally, the penalty for unmet demand in each area is proportional to the amount of unmet demand and the penalty for each unit of unmet demand in that area. Hence, the total penalty for unmet demand C^u over all the areas is:

$$C^u = \sum_i P_i q_i. \quad (8)$$

Define $h_j = f_j (1 - l_j^0) + s_j$. Also, ρ is a weighting factor that balances the first-stage cost and second-stage cost. The two-stage RO problem of the SP can be written as follows:

$$\begin{aligned} (\mathcal{P}_1) : & (1 - \rho) \min_{y,t,x} \sum_j p_j y_j + \sum_j h_j t_j + \beta \sum_{i,j} d_{i,j} x_{i,j} \\ & + \rho \max_{(\lambda,z) \in \Xi} \min_{w,q} \sum_i P_i q_i + \beta \sum_{i,j} d_{i,j} w_{i,j} \end{aligned} \quad (9a)$$

$$\text{s.t. } \Omega_1(\mathbf{x}, \mathbf{y}, \mathbf{t}) = \left\{ \sum_j x_{i,j} \geq \lambda_i^f, \forall i \right\} \quad (9b)$$

$$\sum_j p_j y_j + \sum_j h_j t_j \leq B, \quad (9c)$$

$$\sum_i x_{i,j} \leq y_j \leq C_j t_j \quad \forall j; \quad y_j \in \mathbb{Z}, \quad \forall j \quad (9d)$$

$$0 \leq x_{i,j} \leq a_{i,j} C_j, \quad \forall i, j; \quad t_j \in \{0, 1\}, \quad \forall j \quad (9e)$$

$$\Omega_2(\mathbf{y}, \mathbf{t}, \mathbf{z}, \lambda) = \left\{ \sum_i w_{i,j} \leq y_j t_j (1 - z_j), \quad \forall j \right\} \quad (9f)$$

$$\sum_j w_{i,j} + q_i \geq \lambda_i, \quad \forall i \quad (9g)$$

$$w_{i,j} \leq a_{i,j} C_j, \quad \forall i, j \quad (9h)$$

$$w_{i,j} \geq 0, \quad \forall i, j; \quad q_i \geq 0, \quad \forall i; \quad (\mathbf{z}, \lambda) \in \Xi \quad (9i)$$

The objective of the SP is to minimize the weighted sum of the first-stage cost and the second-stage cost. The first term

in the first stage expresses the total computing resource cost. The second term is the total of the service placement cost and storage cost. The last term in the first stage is the total delay cost. The second-stage cost consists of the penalty cost for unmet demand and the actual delay cost, respectively. Note that the objective function (9a) can be written as:

$$\min_{y,t,x} \left\{ (1-\rho) \left[\sum_j p_j y_j + \sum_j h_j t_j + \beta \sum_{i,j} d_{i,j} x_{i,j} \right] + \max_{(\lambda,z) \in \Xi} \min_{w,q} \rho \left[\sum_i P_i q_i + \beta \sum_{i,j} d_{i,j} w_{i,j} \right] \right\}. \quad (10)$$

Thus, problem (P_1) is indeed a trilevel optimization problem. The first level represents the problem of the SP before the the uncertainties are revealed, which seeks to minimize the SP's cost. The second level represents the worst-case realization of the uncertainties z and λ , which tries to degrade the service quality (i.e., higher delay and more unmet demand) and maximizes the SP's cost. The third level represents the optimal workload allocation problem to mitigate the effects of the uncertainty realization.

The proposed two-stage robust model can be interpreted as follows. In the first stage, the SP minimizes the total cost based on the forecast demand information. In the second stage, the SP optimizes the cost under the worst-case scenario of the uncertainties. The two stages are interdependent through the service provisioning decision in the first stage. The weighting factor ρ reflects the SP's attitude towards the risk of demand fluctuation and node failures in the actual operation stage (i.e., the second stage). A larger value of ρ implies the SP is more conservative and willing to pay more for the resource provisioning cost in the first stage to mitigate the risk of dropping requests and increasing delay due to the system uncertainties in the operation stage.

Let $\Omega_1(x, y, t)$ be the set of constraints related to the first stage. Also, $\Omega_2(y, t, z, \lambda)$ expresses all constraints in the second stage. In particular, constraint (9b) indicates that the total computing resource allocated to each area i must be sufficient to serve the forecast demand in that area. The budget constraint of the SP is presented in (9c). The payment (i.e., provisioning cost) equals to the total cost of service placement and resource procurement, which cannot exceed the SP's budget. Note that β and P_i are used to control the delay and the amount of unmet demand. It is easy to see that the resource provisioning cost tends to increase as β and P_i increase. The delay cost and penalty cost for unmet demand are virtual costs that the SP does not have to pay.

Constraint (9d) enforces that the total amount of resource allocated from each EN j to all areas cannot exceed the amount of purchased resource y_j at that node. Furthermore, the SP should purchase resource only from the ENs at which the service is installed (i.e., $t_j = 1$). Also, the purchased amount is limited by the capacity C_j of the EN. The workload allocation decisions are nonnegative and the placement variables are binary variables as shown in (9e).

In the second stage, we can only allocate resources from ENs that have installed the service (i.e., $t_j = 1$) and are not in a failure state (i.e., $z_j = 0$). Moreover, the total amount of resource allocated from an EN j cannot exceed the procured amount y_j at that node in the first stage. These aspects are captured precisely by constraint (9f). It is easy to see that

the workload initially assigned to a disrupted EN should be reallocated to other non-disrupted ENs. Since y_j serves as a parameter in the second stage, it can be observed that there exists bilinear terms $t_j(1 - z_j)$ in the inner *maxmin* problem. To avoid this bilinear term, we can equivalently reformulate (9f) using the following linear constraints:

$$\sum_i w_{i,j} \leq C_j t_j (1 - z_j); \quad \sum_i w_{i,j} \leq y_j, \quad \forall j. \quad (11)$$

Constraint (9g) represents that the resource demand in each area can either be served by some ENs or be dropped (i.e., q_i). The demand from area i can be served by an EN j only if $a_{i,j} = 1$, which is shown in (9h). Finally, constraint (9i) enforces the feasible regions for the second-stage variables and the uncertainty parameters.

It is worth emphasizing that the main goal of our proposed model is to find the optimal service placement and resource procurement decisions, which need to be determined before the uncertainties are disclosed. These first-stage decisions y and t are robust against any realization of the uncertainties. In practice, the proposed system can be implemented as follows. The SP first solves problem (P_1) to obtain the optimal values of y^* and t^* . After observing the actual realization of the demand λ^a and failures z^a , which is not necessarily the worst-case realization, the SP solves the following problem to obtain the optimal resource allocation decisions w and q in the actual operation stage:

$$\min_{w,q} \quad \sum_i P_i q_i + \beta \sum_{i,j} d_{i,j} w_{i,j} \quad (12a)$$

$$\text{s.t. :} \quad \sum_i w_{i,j} \leq y_j^* t_j^* (1 - z_j^a), \quad \forall j \quad (12b)$$

$$\sum_j w_{i,j} + q_i \geq \lambda_i^a, \quad \forall i \quad (12c)$$

$$w_{i,j} \leq a_{i,j} C_j, \quad \forall i, j \quad (12d)$$

$$w_{i,j} \geq 0, \quad \forall i, j; \quad q_i \geq 0, \quad \forall i. \quad (12e)$$

3 SOLUTION APPROACHES

In this section, we present three solution approaches, including two variants of the CCG algorithm [4] and an affine decision rule (ADR) approximation approach, to solve the formulated trilevel problem (P_1) . First, we can show that (P_1) can be written as a large-scale MILP by enumerating over the set of extreme points of the uncertainty set Ξ . Specifically, if the innermost minimization problem in (P_1) is feasible, we can solve its dual maximization problem instead. Hence, we write the second-stage bilevel problem as a max-max problem, which is simply a maximization problem, over z, λ and dual variables associated with the constraints of the innermost problem. Because the resulting linear maximization problem is optimized over two disjoint polyhedrons, the optimal solution of the second-stage problem occurs at an extreme point of set Ξ .

Let $\Xi^e = \{\xi^1, \xi^2, \dots, \xi^K\}$ be the set of K extreme points of Ξ , where $\xi^l = (\lambda^l, z^l)$ is the l -th extreme point of set Ξ . Note that $\lambda^l = (\lambda_1^l, \lambda_2^l, \dots, \lambda_J^l)$ and $z^l = (z_1^l, z_2^l, \dots, z_J^l)$. Then, problem (P_1) is equivalent to:

$$(1-\rho) \min_{y,t,x \in \Omega_1(x,y,t)} \sum_j p_j y_j + \sum_j h_j t_j + \beta \sum_{i,j} d_{i,j} x_{i,j} + \rho \max_{(\lambda,z) \in \Xi^e} \min_{(w,q) \in \Omega_2(y,t,z,\lambda)} \sum_i P_i q_i + \beta \sum_{i,j} d_{i,j} w_{i,j}. \quad (13)$$

By enumerating all extreme points of Ξ^e , it is easy to see that this problem is equivalent to the following MILP:

$$\min_{\eta, x, y, t} (1 - \rho) \left\{ \sum_j p_j y_j + \sum_j h_j t_j + \beta \sum_{i,j} d_{i,j} x_{i,j} \right\} + \rho \eta \quad (14a)$$

$$\text{s.t. } \eta \geq \sum_i P_i q_i^l + \beta \sum_{i,j} d_{i,j} w_{i,j}^l, \forall l \leq K \quad (14b)$$

$$(w^l, q^l) \in \Omega_2(y, t, z^l, \lambda^l), \forall l \leq K. \quad (14c)$$

When Ξ contains a large number of extreme points, solving this MILP may be not practically feasible. Instead of solving the full equivalent problem (14) for all extreme points in Ξ , we can try to solve this problem for a subset of Ξ^e . Clearly, this relaxed problem contains only a subset of constraints of the minimization problem (14). Thus, this relaxed problem gives us a lower bound (LB) for the optimal value of problem (14). By gradually adding more constraints (i.e., more extreme points) to the relaxed problem, we can improve the LB of the original problem (\mathcal{P}_1). This is indeed the core idea behind the CCG method [4] which allows us to solve (\mathcal{P}_1) without explicitly solving problem (14).

3.1 Column-and-Constraint Generation (CCG)

To solve (\mathcal{P}_1), we first develop an iterative algorithm based on the CCG method [4] that decomposes the original two-stage robust problem into a master problem (**MP**), which is a relaxation of problem (14), and a bilevel max-min subproblem representing the second stage. The optimal value of the **MP** provides a LB while the optimal solution to the subproblem helps us compute an upper bound (UB) for the optimal value of the original problem. Also, the optimal solution to the subproblem provides a significant extreme point that is used to update the **MP**. The optimal solution y and t of the **MP** is used to update the subproblem. By iteratively solving an updated **MP** and a modified subproblem, the UB and LB are improved after every iteration. Thus, CCG is guaranteed to converge to the optimal solution of the original problem in a finite number of iterations.

3.1.1 Master Problem

Initially, the **MP** contains no extreme points. A new extreme point is added to the **MP** at every iteration. Thus, at iteration k , the **MP** has k extreme points and can be written as:

$$\min_{x, y, t, \eta} (1 - \rho) \left\{ \sum_j p_j y_j + \sum_j h_j t_j + \beta \sum_{i,j} d_{i,j} x_{i,j} \right\} + \rho \eta \quad (15a)$$

$$\text{s.t. } (9b) - (9e)$$

$$\eta \geq \sum_i P_i q_i^l + \beta \sum_{i,j} d_{i,j} w_{i,j}^l, \forall l \leq k \quad (15b)$$

$$\sum_i w_{i,j}^l \leq y_j, \forall j \quad (15c)$$

$$\sum_i w_{i,j}^l \leq C_j t_j (1 - z_j^{l,*}), \forall j, l \leq k \quad (15d)$$

$$\sum_j w_{i,j}^l + q_i^l \geq \lambda_i^{l,*}, \forall l \leq k \quad (15e)$$

$$0 \leq w_{i,j}^l \leq a_{i,j} C_j, \forall i, j, l \leq k; \quad q_i^l \geq 0, \forall i, l \leq k, \quad (15f)$$

where $\{(\lambda^{1,*}, z^{1,*}), (\lambda^{2,*}, z^{2,*}), \dots, (\lambda^{k,*}, z^{k,*})\}$ is the set of optimal solutions to the subproblem in all previous iterations up to iteration k . Note that $z^{l,*} = (z_1^{l,*}, z_2^{l,*}, \dots, z_J^{l,*})$ and $\lambda^{l,*} = (\lambda_1^{l,*}, \lambda_2^{l,*}, \dots, \lambda_I^{l,*}), \forall l$. Clearly, the problem in (15) is an MILP. The optimal solution to this **MP** includes the optimal service placement $(t_j^{k+1,*}, \forall j)$, resource procurement $(y_j^{k+1,*}, \forall j)$, second-stage cost $(\eta^{k+1,*})$, workload allocation $(x_{i,j}^{k+1,*}, \forall i, j)$, as well as $w^{l,*}$ and $q^{l,*}, \forall l \leq k$. The optimal service placement and resource procurement decisions $y^{*,k+1}$ and $t^{*,k+1}$ will serve as input to the subproblem described in Section 3.1.2. The **MP** contains only a subset of constraints of the problem (14), which is equivalent to the original problem (\mathcal{P}_1). Hence, the optimal value of the **MP** is a LB for the optimal value of the original problem. The LB achieved after solving the **MP** at iteration k is:

$$LB = (1 - \rho) \left\{ \sum_j p_j y_j^{k+1,*} + \sum_j h_j t_j^{k+1,*} + \beta \sum_{i,j} d_{i,j} x_{i,j}^{k+1,*} \right\} + \rho \eta^{k+1,*}. \quad (16)$$

3.1.2 Subproblem

The subproblem is a bilevel max-min problem representing the decision making process of the SP in the second stage. Specifically, given the first-stage decisions y and t , the subproblem is given as follows:

$$\mathcal{Q}(y, t) = \rho \max_{(\lambda, z) \in \Xi} \min_{(w, q) \in \Omega_2(y, t, z, \lambda)} \sum_i P_i q_i + \beta \sum_{i,j} d_{i,j} w_{i,j}. \quad (17)$$

The inner problem can be written explicitly as:

$$\min_{w, q} \sum_i P_i q_i + \beta \sum_{i,j} d_{i,j} w_{i,j} \quad (18a)$$

$$\text{s.t. } \sum_i w_{i,j} \leq C_j t_j (1 - z_j), \forall j \quad (u_j^1) \quad (18b)$$

$$\sum_i w_{i,j} \leq y_j, \forall j \quad (u_j^2) \quad (18c)$$

$$\sum_j w_{i,j} + q_i \geq \lambda_i, \forall i \quad (s_i) \quad (18d)$$

$$w_{i,j} \leq a_{i,j} C_j, \forall i, j \quad (\pi_{i,j}) \quad (18e)$$

$$w_{i,j} \geq 0, \forall i, j; \quad q_i \geq 0, \forall i, \quad (18f)$$

where u_j^1, u_j^2, s_i , and $\pi_{i,j}$ are dual variables associated with the corresponding constraints. Also, t and y in problem (18) are the optimal placement and procurement to the latest **MP**. Thus, at iteration k , for the subproblem, we have $t_j = t_j^{k+1,*}$ and $y_j = y_j^{k+1,*}, \forall j$. It can be observed that problem (18) is feasible for any uncertainty realization (λ, z) as well as any values of y and t because $(w_{i,j} = 0, \forall i, j, q_i = \lambda_i, \forall i)$ is always a feasible solution to this problem. Therefore, the second-stage problem satisfies the *relatively complete recourse* condition that is required for CCG [4] to work. The relatively complete recourse condition implies that the second-stage problem is feasible for any given values of the uncertainty realization as well as the service placement and resource procurement computed by the **MP**.

The subproblem is a bilevel max-min problem, which is difficult to solve. To make it easier to follow the CCG method, we temporarily assume that there is an oracle that

can output an optimal solution to problem (17) for any given values of y and t . We will present two approaches to solve the subproblem later. Let $(z^{k+1,*}, \lambda^{k+1,*}, w^{k+1,*}, q^{k+1,*})$ be an optimal solution to the subproblem at iteration k . Then, $z^{k+1,*}$ and $\lambda^{k+1,*}$ are used as input to the **MP** in the next iteration. Also, the UB for the optimal value of the original problem (\mathcal{P}_1) can be updated as follows:

$$UB^{k+1} = (1 - \rho) \left\{ \sum_j p_j y_j^{k+1,*} + \sum_j h_j t_j^{k+1,*} \right. \quad (19a)$$

$$\left. + \beta \sum_{i,j} d_{i,j} x_{i,j}^{k+1,*} \right\} + \rho \left\{ \sum_i P_i q_i^{k+1,*} + \beta \sum_{i,j} d_{i,j} w_{i,j}^{k+1,*} \right\},$$

$$UB = \min \{ UB, UB^{k+1} \}. \quad (19b)$$

3.1.3 CCG-based Iterative Algorithm

Based on the description of the **MP** and the subproblem above, we are now ready to present the CCG algorithm for solving the two-stage robust edge service placement and workload allocation problem (\mathcal{P}_1) in an iterative master-subproblem framework, as shown in **Algorithm 1**.

Algorithm 1 CCG-based Iterative Algorithm

- 1: Initialization: set $k = 0$, $LB = -\infty$, and $UB = +\infty$.
 - 2: **repeat**
 - 3: Solve the **MP** in (15) to obtain an optimal solution $(x^{k+1,*}, y^{k+1,*}, t^{k+1,*}, \eta^{k+1,*})$ and update LB according to (16).
 - 4: Solve the subproblem (17) with $t = t^{k+1,*}$ and $y = y^{k+1,*}$ to obtain an extreme point $(z^{k+1,*}, \lambda^{k+1,*})$ and update UB following (19).
 - 5: Update $z^{k+1} = z^{k+1,*}$ and $\lambda^{k+1} = \lambda^{k+1,*}$, which are used to create new cuts in the **MP** in the next iteration. Also, update $k = k + 1$. Go to Step 3.
 - 6: **until** $\frac{UB-LB}{UB} \leq \epsilon$
 - 7: Output: optimal placement and resource procurement decisions (t^*, y^*) .
-

The CCG algorithm starts by solving an **MP** in Step 3 to find an optimal placement and procurement solution, which will serve as input to the subproblem in Step 4. The subproblem gives us a new extreme point, which represents the worst-case uncertainty scenario for the given optimal y and t in Step 3. This extreme point is used to generate new cuts (i.e., new constraints) to add to the **MP** in the next iteration. Since new constraints related to the uncertainties z and λ are added to the **MP** at every iteration, the feasible region of the **MP** decreases. Hence, the LB is weakly-increasing (i.e., improved) after each iteration. By definition in (19), the UB is non-increasing. Furthermore, since Ξ^e is a finite set with K elements while the subproblem produces a new extreme point at every iteration, **Algorithm 1** will converge in a finite number of iterations.

Proposition 3.1. *Algorithm 1 converges to the optimal solution to the original problem (\mathcal{P}_1) in $O(K)$ iterations.*

Proof. Please refer to Appendix 7.1 for more details. \square

In CCG, we need to solve a bilevel max-min subproblem at every iteration. In **Algorithm 1**, we assume that there is an oracle to solve the subproblem (17). In the following,

we present two approaches to implement this oracle. The first approach follows the original CCG paper [4] that uses KKT conditions to transform the bilevel subproblem into an equivalent MILP. When the demand uncertainty budget Γ is an integer, we propose an alternative approach that converts the subproblem to an MILP by using LP duality. The resulting MILP from the duality-based approach has significantly less number of constraints and integer variables compared to the MILP obtained by the KKT conditions.

3.1.4 KKT-based Solution for the Subproblem

Similar to the CCG algorithm in [4], we can use KKT conditions to transform the subproblem (17) into an equivalent MILP problem. The KKT conditions are applied to the innermost problem (18). The resulting set of KKT conditions contains stationarity, primal feasibility, dual feasibility, complementary slackness constraints. Each non-linear complementary constraint can be transformed into a set of linear constraints by using Fortuny-Amat transformation [8]. Please also refer to Appendix 7.2 for more details. The final reformulation of the subproblem (17) through KKT conditions is an MILP, which is shown as follows.

$$\max_{(z,\lambda) \in \Xi, w, q} \rho \left\{ \sum_i P_i q_i + \beta \sum_{i,j} d_{i,j} w_{i,j} \right\} \quad (20a)$$

$$\text{s.t. } 0 \leq w_{i,j} \leq M_{i,j}^1 (1 - v_{i,j}^1), \forall i, j \quad (20b)$$

$$0 \leq \rho P_i d_{i,j} + \pi_{i,j} + u_j^1 + u_j^2 - s_i \leq M_{i,j}^1 v_{i,j}^1, \forall i, j \quad (20c)$$

$$0 \leq \rho P_i - s_i \leq M_i^2 v_i^2, \forall i \quad (20d)$$

$$0 \leq q_i \leq M_i^2 (1 - v_i^2), \forall i \quad (20e)$$

$$0 \leq C_j \hat{t}_j (1 - z_j) - \sum_i w_{i,j} \leq M_j^3 v_j^3, \forall j \quad (20f)$$

$$0 \leq u_j^1 \leq M_j^3 (1 - v_j^3), \forall j \quad (20g)$$

$$0 \leq \hat{y}_j - \sum_i w_{i,j} \leq M_j^4 v_j^4, \forall j \quad (20h)$$

$$0 \leq u_j^2 \leq M_j^4 (1 - v_j^4), \forall j \quad (20i)$$

$$0 \leq \sum_j w_{i,j} + q_i - \bar{\lambda}_i - g_i \tilde{\lambda}_i \leq M_i^5 v_i^5, \forall i \quad (20j)$$

$$0 \leq s_i \leq M_i^5 (1 - v_i^5), \forall i \quad (20k)$$

$$0 \leq a_{i,j} C_{i,j} - w_{i,j} \leq M_{i,j}^6 v_{i,j}^6, \forall i, j \quad (20l)$$

$$0 \leq \pi_{i,j} \leq M_{i,j}^6 (1 - v_{i,j}^6), \forall i, j \quad (20m)$$

$$v_{i,j}^1, v_{i,j}^6 \in \{0, 1\}, \forall i, j \quad (20n)$$

$$v_i^2, v_i^5 \in \{0, 1\}, \forall i; v_j^3, v_j^4 \in \{0, 1\}, \forall j, \quad (20o)$$

where $M_{i,j}^1, M_i^2, M_j^3, M_j^4, M_i^5$ and $M_{i,j}^6$ are sufficiently large numbers.

3.1.5 Duality-based Solution for the Subproblem

Instead of the KKT-based reformulation as in [4], when the demand uncertainty budget Γ is an integer, we can transform the subproblem into an MILP using duality-based reformulation. If Γ is non-integer, the SP can round it up to the closest integer, which indeed slightly enlarges the uncertainty set \mathcal{D} and makes the optimal solution more robust. Thus, restricting Γ to be an integer is a mild assumption. Compared to the KKT-based reformulation, the duality-based reformulation has the advantage of generating fewer variables and constraints, which reduces computational time, especially for large-scale systems. By using LP duality,

we first write the dual of (18) and then, the subproblem (17) becomes a max-max problem (i.e., simply a maximization problem). Hence, the subproblem (17) is equivalent to:

$$\rho \max_{u^1, u^2, s, \pi, g, z} \left\{ \sum_i \bar{\lambda}_i s_i + \sum_i \tilde{\lambda}_i s_i g_i - \sum_j C_j t_j (1 - z_j) u_j^1 - \sum_j y_j u_j^2 - \sum_{i,j} a_{i,j} C_j \pi_{i,j} \right\} \quad (21a)$$

$$\text{s.t. } s_i \leq P_i, \quad \forall i \quad (21b)$$

$$s_i - u_j^1 - u_j^2 - \pi_{i,j} \leq \beta d_{i,j}, \quad \forall i, j \quad (21c)$$

$$u_j^1, u_j^2 \geq 0, \quad \forall j; \quad s_i \geq 0, \quad \forall i \quad (21d)$$

$$\sum_j z_j \leq K; \quad z_j \in \{0, 1\}, \quad \forall j \quad (21e)$$

$$\sum_j g_i \leq \Gamma; \quad 0 \leq g_i \leq 1, \quad \forall i. \quad (21f)$$

Note that $\lambda = \bar{\lambda}_i + \tilde{\lambda}_i g_i$ from (1). Also, y and t are parameters in problem (21). Due to the bilinear terms $s_i g_i$ and $z_j u_j^1$, (21) is a non-linear optimization problem. Since the term $z_j u_j^1$ is a product of a binary variable and a continuous variable, we can linearize it as follows. Define $U_j = z_j u_j^1$. Then, the bilinear term $z_j u_j^1$ can be replaced by U_j and the following linear equations: $U_j \leq u_j^1, \forall j$; $U_j \leq M z_j, \forall j$; $U_i \geq u_j^1 - M(1 - z_j), \forall j$; $U_i \geq 0$, where M is a sufficiently large number. Furthermore, since Γ is an integer, it is easy to see that there always exists an optimal solution where $g_i \in \{0, 1\}, \forall i$. Then, the bilinear term $s_i g_i$ becomes a product of a continuous variable and a binary variable. Thus, similar to $z_j u_j^1$, we can linearize $s_i g_i$ using a set of equivalent linear equations. Let $v_i = s_i g_i, \forall i$. Then, instead of solving the non-linear problem (21), we can solve the following MILP:

$$\rho \max_{u^1, u^2, s, \pi, g, z} \left\{ \sum_i \bar{\lambda}_i s_i + \sum_i \tilde{\lambda}_i v_i + \sum_j C_j t_j U_j - \sum_j C_j t_j u_j^1 - \sum_j y_j u_j^2 - \sum_{i,j} a_{i,j} C_j \pi_{i,j} \right\} \quad (22a)$$

$$\text{s.t. } s_i \leq P_i, \quad \forall i; \quad s_i - u_j - \pi_{i,j} \leq \beta d_{i,j}, \quad \forall i, j \quad (22b)$$

$$v_i \leq s_i, \quad \forall i; \quad v_i \leq M g_i, \quad \forall i; \quad v_i \geq s_i - M(1 - g_i), \quad \forall i \quad (22c)$$

$$U_j \leq u_j^1, \quad \forall j; \quad U_j \leq M z_j, \quad \forall j \quad (22d)$$

$$U_i \geq u_j^1 - M(1 - z_j), \quad \forall j \quad (22e)$$

$$u_j^1, u_j^2, U_j \geq 0, \quad \forall j; \quad v_i, s_i \geq 0, \quad \forall i; \quad \pi_{i,j} \geq 0, \quad \forall i, j \quad (22f)$$

$$\sum_j z_j \leq K; \quad z_j \in \{0, 1\}; \quad \sum_i g_i \leq \Gamma, \quad g_i \in \{0, 1\}, \quad \forall i. \quad (22g)$$

When we use the duality-based transformation to solve the subproblem (17), instead of using (19), we can update the UB at iteration k as follows:

$$UB^{k+1} = (1 - \rho) \left\{ \sum_j p_j y_j^{k+1,*} + \sum_j h_j t_j^{k+1,*} + \beta \sum_{i,j} d_{i,j} x_{i,j}^{k+1,*} \right\} + \rho \left\{ \sum_i \bar{\lambda}_i s_i^* + \sum_i \tilde{\lambda}_i v_i^* + \sum_j C_j t_j U_j^* - \sum_j C_j t_j u_j^{1,*} - \sum_j y_j u_j^{2,*} - \sum_{i,j} a_{i,j} C_j \pi_{i,j}^* \right\} \quad (23a)$$

$$UB = \min \{UB, UB^{k+1}\}, \quad (23b)$$

where $(s^*, v^*, U^*, u^{1,*}, u^{2,*}, \pi^*)$ is an optimal solution to problem (22).

3.2 Affine Decision Rule (ADR) Approach

Although CCG can give an optimal solution to problem (P_1) within a finite number of iterations, its computational time depends on the size of the uncertainty set. From Proposition 3.1, the computational time is sensitive to the number of extreme points of the uncertainty set Ξ , i.e., the number of element of Ξ^e . In the worst-case, it can take a long time to converge if the uncertainty set has a huge number of extreme points. Hence, we propose an affine decision rule (ADR) approximation approach [5]–[7], which is insensitive to the set size, to solve large-scale problem instances.

The main idea behind ADR is to restrict the second-stage variables (i.e., recourse variables) to be affine functions of the uncertain data. If these functions are given, then for any realization of the uncertainties, we can simply use them to compute the suboptimal recourse decisions. Thus, the goal of ADR is to find reasonable functions to approximate the optimal solution to the original robust problem. While ADR only provides a suboptimal solution, Kuhn *et al.* showed that ADR performs surprisingly well on many practical problems and it is even optimal in certain problem classes [7]. This motivates us to examine the performance of ADR for our two-stage robust problem (P_1) .

Let $q_i(\lambda, z)$ and $w_{i,j}(\lambda, z)$ express q_i and $w_{i,j}$ as functions of the uncertainties λ and z . Then, the original problem (P_1) can be written as follows:

$$(P'_1): (1 - \rho) \min_{y, t, x} \sum_j p_j y_j + \sum_j h_j t_j + \beta \sum_{i,j} d_{i,j} x_{i,j} + \rho \max_{(\lambda, z) \in \Xi} \min_{w, q} \sum_{i \in I} P_i q_i(\lambda, z) + \beta \sum_{i,j} d_{i,j} w_{i,j}(\lambda, z) \quad (24a)$$

$$\text{s.t. } x, y, t \in \Omega_1(x, y, t) \quad (24b)$$

$$\sum_i w_{i,j}(\lambda, z) \leq C_j t_j (1 - z_j), \quad \forall j, \quad \forall (\lambda, z) \in \Xi \quad (24c)$$

$$\sum_i w_{i,j}(\lambda, z) \leq y_j, \quad \forall j, \quad \forall (\lambda, z) \in \Xi \quad (24d)$$

$$\sum_j w_{i,j}(\lambda, z) + q_i(\lambda, z) \geq \lambda_i, \quad \forall i, \quad \forall (\lambda, z) \in \Xi \quad (24e)$$

$$0 \leq w_{i,j}(\lambda, z) \leq a_{i,j} C_j, \quad \forall i, j, \quad \forall (\lambda, z) \in \Xi \quad (24f)$$

$$q_i(\lambda, z) \geq 0, \quad \forall i; \quad \forall (\lambda, z) \in \Xi. \quad (24g)$$

In ADR, the second-stage variables $w_{i,j}$ and q_i are defined as affine functions of the uncertainties λ and z . Thus:

$$w_{i,j}(\lambda, z) = \sum_{e \in \mathcal{I}} A_{i,j}^e \lambda_e + \sum_{l \in \mathcal{J}} B_{i,j}^l z_l + D_{i,j}, \quad \forall i, j \quad (25)$$

$$q_i(\lambda, z) = \sum_{e \in \mathcal{I}} E_i^e \lambda_e + \sum_{l \in \mathcal{J}} F_i^l z_l + G_i, \quad \forall i, \quad (26)$$

where e is area index and l is EN index. Also, $A_{i,j}^e, B_{i,j}^l, D_{i,j}, E_i^e, F_i^l$ and $G_i \in \mathbb{R}$. It can be observed that, for each realization of the uncertain data λ and z , we can readily compute the value of w and q by using (25) and (26). Thus, the objective of the ADR approach is to optimize the coefficients $A_{i,j}^e, B_{i,j}^l, D_{i,j}, E_i^e, F_i^l$ and G_i in (25) and (26).

By using the ADR (25) and (26) and the epigraph form for (\mathcal{P}'_1) , we obtain the following ADR model (27) for (\mathcal{P}_1) :

$$(\mathcal{P}_1^{\text{ADR}}) : (1 - \rho) \min_{x,y,t, A,B,D,E,F,G} \left\{ \sum_j p_j y_j + \sum_j h_j t_j + \beta \sum_{i,j} d_{i,j} x_{i,j} + \rho \phi \right\} \quad (27a)$$

$$\text{s.t. } x, y, t \in \Omega_1(x, y, t) \quad (27b)$$

$$\phi \geq \sum_i P_i \left(\sum_e E_i^e \lambda_e + \sum_l F_i^l z_l + G_i \right) + \quad (27c)$$

$$+ \beta \sum_{i,j} d_{i,j} \left(\sum_e A_{i,j}^e \lambda_e + \sum_l B_{i,j}^l z_l + D_{i,j} \right), \forall (\lambda, z) \in \Xi$$

$$\sum_i \left(\sum_e A_{i,j}^e \lambda_e + \sum_l B_{i,j}^l z_l + D_{i,j} \right) \leq C_j t_j (1 - z_j), \quad \forall j, \forall (\lambda, z) \in \Xi \quad (27d)$$

$$\sum_i \left(\sum_e A_{i,j}^e \lambda_e + \sum_l B_{i,j}^l z_l + D_{i,j} \right) \leq y_j, \quad \forall j, \forall (\lambda, z) \in \Xi \quad (27e)$$

$$\sum_j \left(\sum_e A_{i,j}^e \lambda_e + \sum_l B_{i,j}^l z_l + D_{i,j} \right) + \left(\sum_e E_i^e \lambda_e + \sum_l F_i^l z_l + G_i \right) \geq \lambda_i, \quad \forall i, \forall (\lambda, z) \in \Xi \quad (27f)$$

$$\sum_e E_i^e \lambda_e + \sum_l F_i^l z_l + G_i \geq 0, \quad \forall i, \forall (\lambda, z) \in \Xi \quad (27g)$$

$$\sum_e A_{i,j}^e \lambda_e + \sum_l B_{i,j}^l z_l + D_{i,j} \geq 0, \quad \forall i, j, \forall (\lambda, z) \in \Xi \quad (27h)$$

$$\sum_e A_{i,j}^e \lambda_e + \sum_l B_{i,j}^l z_l + D_{i,j} \leq a_{i,j} C_j, \quad \forall i, j, \forall (\lambda, z) \in \Xi. \quad (27i)$$

To solve the ADR model (27), we first need to convert each robust constraint into a solvable form. Specifically, we employ LP duality to reformulate each robust constraint into an equivalent set of linear equations. Due to space limitation, please refer to *Appendix 7.3* for more details. After converting each robust constraint into a set of linear equations, we obtain the following MILP:

$$(1 - \rho) \min_{x,y,t, A,B,D,E,F,G} \sum_j p_j y_j + \sum_j h_j t_j + \beta \sum_{i,j} d_{i,j} x_{i,j} + \rho \phi \quad (28)$$

$$\text{s.t. } x, y, t \in \Omega_1(x, y, t) \quad (28)$$

(39) – (45) in *Appendix 7.3*.

Although the ADR approach only gives us a suboptimal solution, our numerical results show that the ADR solution is quite close to the exact optimal solution. Thus, it provides a good approximation scheme for our problem. Furthermore, for some special cases, we can show that the ADR approach generates an exact optimal first-stage decision for the original problem (\mathcal{P}_1) . Note that we only care about the first-stage decisions because in the operation stage, the SP will eventually reoptimize the second-stage decisions by solving LP problem (12) after the uncertainties are revealed.

We have the following proposition in regards to the optimality of the ADR approach.

Proposition 3.2 (Optimality of Affine Decision Rule [5]). *If the uncertainty set Ξ is a simplex (i.e., the convex hull of its vertices), the affine policy can give an optimal first-stage solution.*

From *Proposition 3.2*, we can show that there exists some special cases where the ADR approach gives an optimal solution to the original problem (\mathcal{P}_1) . For example, consider the case where $K = 0$ and $\Gamma = 1$. In other words, the SP considers only demand uncertainty and set Ξ is the same as set \mathcal{D} . Also, $\sum_{i \in \mathcal{I}} g_i \leq 1$. Let $g_0 \geq 0$ be a slack variable such that $g_0 + \sum_{i \in \mathcal{I}} g_i = 1$. We consider the following $I + 1$ vertices of Ξ (i.e., \mathcal{D}): $(\bar{\lambda}_1, \bar{\lambda}_2, \dots, \bar{\lambda}_I)$, $(\bar{\lambda}_1 + \tilde{\lambda}_1, \bar{\lambda}_2, \dots, \bar{\lambda}_I)$, $(\bar{\lambda}_1, \bar{\lambda}_2 + \tilde{\lambda}_2, \dots, \bar{\lambda}_I)$, \dots , $(\bar{\lambda}_1, \bar{\lambda}_2, \dots, \bar{\lambda}_I + \tilde{\lambda}_I)$.

Recall from (1), we have $\lambda_i = \bar{\lambda}_i + g_i \tilde{\lambda}_i, \forall i$. Since $g_0 + \sum_{i \in \mathcal{I}} g_i = 1$, it is easy to see that:

$$\begin{aligned} \lambda &= (\bar{\lambda}_1 + g_1 \tilde{\lambda}_1, \bar{\lambda}_2 + g_2 \tilde{\lambda}_2, \dots, \bar{\lambda}_I + g_I \tilde{\lambda}_I) \quad (29) \\ &= g_0 (\bar{\lambda}_1, \bar{\lambda}_2, \dots, \bar{\lambda}_I) + \sum_{i \in \mathcal{I}} g_i (\bar{\lambda}_1, \dots, \bar{\lambda}_i + \tilde{\lambda}_i, \dots, \bar{\lambda}_I). \end{aligned}$$

Hence, the uncertainty set Ξ is a simplex in this case. As a result, from *Proposition 3.2*, ADR gives an optimal solution to problem (\mathcal{P}_1) when $K = 0$ and $\Gamma = 1$. By following similar procedure, we can also show that ADR gives an optimal solution to problem (\mathcal{P}_1) when $K = 1$ and $\Gamma = 0$.

4 NUMERICAL RESULTS

4.1 Simulation Setting

We consider an edge system with 20 areas and each area has an EN (i.e., $I = |\mathcal{I}| = |\mathcal{J}| = J = 20$). We will also perform sensitivity analysis on larger networks with more than 20 areas. Since we are not aware of any public data for edge networks, similar to [2], [10], [12], we adopt the popular Barabasi-Albert model to generate a random scale-free edge network topology. The link delays are generated randomly in the range of [2, 5]ms [2]. Then, the network delay between an AP i and EN j is the delay of the shortest path between them. We assume that all ENs area eligible to serve demand from every area, i.e., $a_{i,j}$ is set to be 1, $\forall i, j$.

Using the hourly price of the *m5d.xlarge* Amazon EC2 instance [30] as a reference, the unit resource prices at the ENs are randomly generated from \$0.02 to \$0.06 per vCPU-hour. Also, the capacities of the ENs are set randomly among 32, 48, and 64 vCPUs. The service placement and storage costs (h_j) are randomly generated between \$0.08 and \$0.1. The budget of the SP is set to be 20. We also assume that the service is not available on any EN at the beginning (i.e., $l_j^0 = 0, \forall j$). By analyzing the trace in [31], we randomly generate the nominal demand in each area between 5 and 40. Also, define α as the ratio between maximum demand deviation $\tilde{\lambda}_i$ and the nominal demand $\bar{\lambda}_i$ (i.e., $\tilde{\lambda}_i = \alpha \bar{\lambda}_i, \forall i$).

In the default setting, $\rho = 0.2$, $\Gamma = 5$, $K = 2$, $\beta = 0.1$, $\alpha = 0.6$, and $P_i = P = 5, \forall i$. We will also vary these parameters when conducting sensitivity analysis. All the experiments are implemented in MATLAB environment using CVX¹ and Gurobi² on a laptop with an Intel Core i7-8700K CPU and 16GB of RAM.

4.2 Performance Evaluation

First, we compare the performance of the proposed two-stage robust (ARO) model (\mathcal{P}_1) with three benchmarks:

1. <http://cvxr.com/cvx/>
2. <https://www.gurobi.com/>

- 1) *Deterministic model (DET)*: see Appendix 7.4. In this model, the SP uses the forecast demand and does not consider EN failures when making decisions.
- 2) *Two-stage stochastic model (SO)*: see Appendix 7.5. This model aims to optimize the expected system performance over a set of scenarios generated from historical data or a certain probability distribution.
- 3) *Heuristic approach (HEU)*: this scheme uses the forecast demand to make the service placement and workload allocation decision. The SP first sorts the areas based on their demands. Then, the workload in each area is allocated one by one, starting from the highest demand area. For each area, the service is placed onto its closest EN and the whole demand of the area is assigned to this EN if this EN has sufficient capacity. Otherwise, a portion of the demand is assigned to this EN and the remaining is allocated to the second-closest EN. This process is repeated until the demand is fully allocated. The usable capacity of each EN is updated during the process.

For the SO scheme, we generate the demand scenarios from a truncated multivariate normal distribution [2]. These (training) scenarios are used as input to the SO model shown in Appendix 7.5. The output of the SO model is the optimal service placement and resource procurement solution (t, y) . Similarly, we solve the deterministic model in Appendix 7.4, the ARO model (P_1) , and run the heuristic scheme to find different optimal service placement and resource procurement solutions. These solutions are computed before the actual operation stage. For all four schemes, given the service placement and resource procurement decisions in the first stage, after observing the actual realization of the demand and the EN failures, the SP will solve the linear problem (12) to determine the actual workload allocation and unmet demand decisions. The *actual total cost* of each scheme is the total of the provisioning cost in the first stage and the actual cost in the operation stage (i.e., second stage).

To compare the performance of these schemes, we use Monte-Carlo simulation and generate 1000 (testing) scenarios to represent the demand and failures in the actual operation stage. Specifically, the actual demand is generated from a (truncated) log-normal distribution [2] and the EN failures are generated randomly from the failure uncertainty set \mathcal{Z} . We have also used other distributions to generate the demand, and observed similar trends and insights for all the figures. In the following, the **average cost** is the expected actual cost from the 1000 generated scenarios, whereas the **worst-case cost** is the highest cost among these scenarios.

Figs. 3(a)-3(b) compare performance of the four schemes when the failure budget K varies. We can find that the actual costs of all the schemes increase when the number of possible failures K increases. Furthermore, ARO significantly outperforms the other schemes. It is because both the demand and failure uncertainties are explicitly captured in ARO. Thus, an ARO solution typically installs the service on more ENs and procures resources more evenly among the selected ENs, which makes it more resilient to unexpected failures of ENs and demand fluctuation. When a failure happens at an EN that has installed the service in the first stage, the workload initially assigned to this node can be reallocated to the other selected ENs.

The SO scheme performs better than the deterministic and heuristic schemes since the SO model takes the uncertainties into account when making the first-stage decisions. However, SO does not consider worst-case uncertainty realization. Moreover, the actual uncertainty realization may not always follow the historical pattern. Hence, SO performs worse than ARO. Define Ψ as the scaling factor for the unmet demand penalty parameter P compared to its value in the default setting. Figs. 3(c)-3(d) further confirm the superior performance of the proposed ARO scheme compared to the other schemes. Additionally, it is easy to see that the total cost increases when the unmet demand penalty P increases. Figs. 3(a)-3(d) show another advantage of ARO is that its cost does not vary too much when K or the unmet demand penalty changes. Therefore, ARO is a preferred method for SPs who require high quality of service.

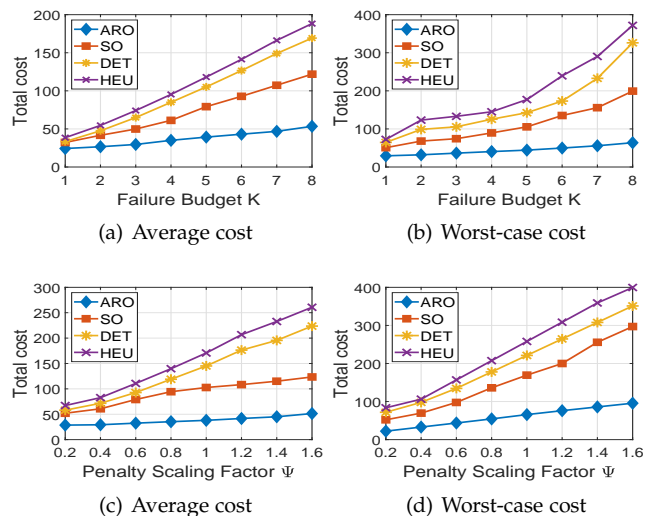


Fig. 3: Performance comparison

To illustrate the benefit of integrating failure uncertainty in the decision-making model of the SP, we will compare the performance of the proposed ARO model *with* and *without* failure consideration. For the case without considering failures, the SP can simply set $K = 0$. For ARO with failure consideration, we set K to be 2 (i.e., the first-stage decisions are robust against up to any two simultaneous failed ENs). Our results show that the provisioning costs with and without considering failures are almost the same. Both schemes almost exhaust the budget. On the other hand, Figs. 4(a)-4(b) show that ARO with failure consideration significantly reduces the SP's cost during node failure events. Although we do not present the result here, the benefit of considering failures (i.e., the gap between two curves in each figure) increase drastically when the unmet demand penalty P increases. Hence, failure consideration is important for SPs who need to maintain high service quality (i.e., less unmet demand).

For ARO with $K = 2$, it can be observed that the cost increases slowly when the number of *actual* failures is small, which implies that a minimal preparation (for $K = 2$) can make the system resilient to unexpected failures. When more than five ENs (i.e., more than 25% of ENs) fail simultaneously, the cost increases faster because the probability that an EN selected for service placement in the first stage fails increases. To hedge against a large number of EN failures,

the SP obviously should set K to be higher. However, it will increase the service provisioning cost. Hence, based on the desired level of robustness and resiliency, the SP needs to decide a proper value for K .

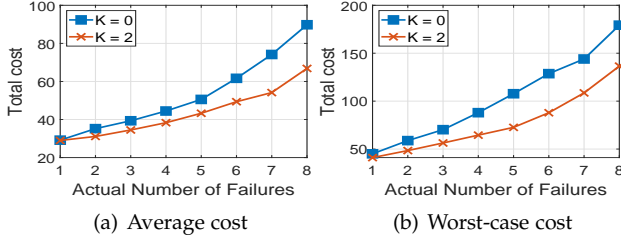


Fig. 4: The advantage of considering failure uncertainty

4.3 Sensitivity Analysis

Now, we evaluate the impacts of important system parameters on the optimal solution. Figs. 5(a)-5(b) illustrate the impacts of the uncertainty set on the system performance. It can be observed that the total cost increases as the uncertainty set enlarges (i.e., when K and Γ increase). Hence, there is an inherent tradeoff between the system cost and the level of robustness. Also, we can see that the system cost increases when ρ increases (i.e., the SP is more risk-averse). Note that “Objective” is the optimal objective value of (\mathcal{P}_1) .

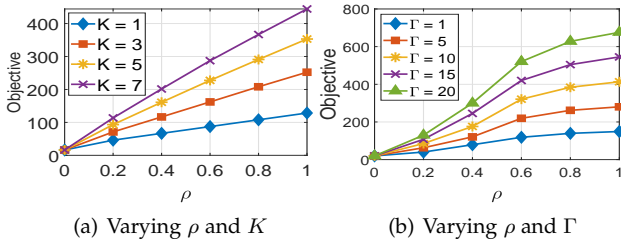


Fig. 5: The impacts of the uncertainty set on the performance

The impacts of the delay penalty parameter β on the optimal solution are presented in Figs. 6(a)-6(b). A higher value of β indicates the service is more delay-sensitive and results in a higher cost. It is because when β is high, the SP will try to allocate the demand in every area to its closest ENs to reduce the delay penalty cost. Thus, cheaper ENs may not be chosen. Fig. 6(a) further shows that the cost increases as ρ increases. Additionally, it can be seen from Fig. 6(b), a higher value of α (i.e., a larger uncertainty set) leads to a higher cost. Indeed, although not shown here, the first-stage provisioning cost also increases when the uncertainty set size, the delay penalty, and ρ increase.

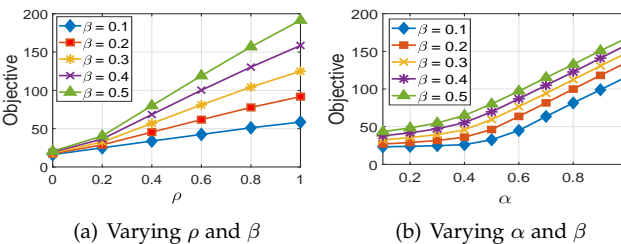


Fig. 6: The impacts of β on the system performance

Finally, we examine the impacts of the system size on the optimal solution. Intuitively, when the number of ENs decreases, the total edge resource capacity is reduced. When the number of areas increases, the total demand in the system increases. As expected, Fig. 7(a) shows that the total cost decreases as the number of ENs increases. The reason is that the SP has more options (i.e., more flexibility) for purchasing resources when more ENs are available. Also, as can be seen in Fig. 7(b), the total cost increases when the number of areas increases. This result is intuitive since the SP needs to procure more resources to serve higher demand.

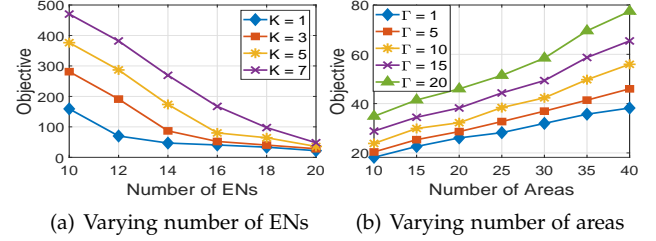


Fig. 7: The impacts of the system size on the performance

4.4 Comparison Between CCG and ADR

4.4.1 Convergence of CCG

Figs. 8(a)-8(b) show the convergence of the CCG algorithm for different values of K and Γ . The algorithm converges within a small number of iterations in both cases. However, the number of iterations increases as K and Γ increase. Note that larger values of K and Γ imply the uncertainty set Ξ has more extreme points. Thus, the convergence of CCG is sensitive to the uncertainty set (i.e., K and Γ here).

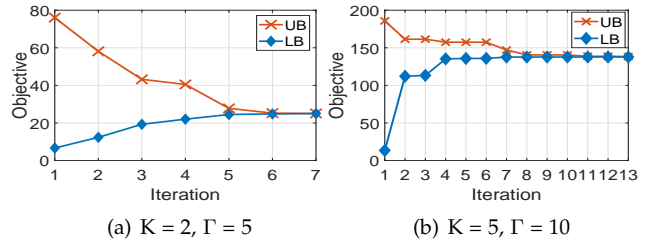


Fig. 8: Convergence of CCG

4.4.2 CCG and ADR

In the following, we analyze and compare the performance of the CCG-based iterative algorithms and the ADR approach. Fig. 9(a) depicts the optimal costs produced by CCG and ADR when we vary the demand uncertainty budget Γ and the failure budget K . Recall that CCG outputs an exact optimal solution for our problem (\mathcal{P}_1) while ADR is an approximation scheme. It is easy to see that the both the total cost and the provisioning cost produced by the ADR policy are quite close to the exact optimal values obtained from the CCG method. Additionally, the optimality gap is small when K is small. In practice, the number of simultaneous failures is typically small, except during extreme events like natural disasters. Indeed, two failures in our setting already corresponds to 10% of nodes fail. Hence, ADR can be an alternative tool for the SP to solve most of the practical cases.

Table 2 reports the running-time of the KKT-based CCG, duality-based CCG, and ADR algorithms for different values of K . We can see that the computational time of the CCG-based algorithms is sensitive to K , thus, it is sensitive to the uncertainty set. On the other hands, ADR is not very sensitive to the uncertainty set because ADR solves an MILP that does not depends on the number of extreme points of Ξ . Also, the KKT-based CCG algorithm is generally slower than the duality-based CCG algorithm since the KKT-based subproblem reformulation has a significantly larger size (in terms of number of constraints and integer variables) compared to the duality-based subproblem reformulation. For example, when $K = 9$, the KKT-based CCG algorithm does not converge after 10 hours.

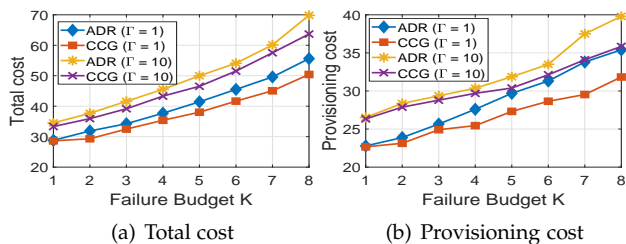


Fig. 9: Comparison between CCG vs ADR

We have also conducted experiments for various values of K and Γ and found that the CCG algorithm normally converges quickly for small values of K and Γ . Also, the duality-based CCG algorithm typically runs faster than the KKT-based CCG algorithm. For large uncertainty sets, instead of CCG, the SP may use ADR to obtain a good approximation solution in a reasonable time. In practice, the SP can run both the duality-based CCG and ADR algorithms in parallel and only implement the solution obtained by the ADR algorithm if the duality-based CCG does not converge after a certain amount of time.

| Running time comparison ($\Gamma = 10$) | | | |
|---|-------------------|---------------|---------|
| K | Duality-based CCG | KKT-based CCG | ADR |
| 5 | 1431.5s | 3387s | 162.87s |
| 7 | 3287s | 11876s | 275.28s |
| 9 | 4416s | NA | 287s |

TABLE 2: Computational time comparison

5 RELATED WORK

Numerous problems in EC have been studied over the last few years. There is a rich literature on edge resource allocation and service placement [10]–[22]. The problem of joint allocation of communication and computational resources for task offloading in mobile EC has attracted significant attention from the wireless community [29]. In [10], [11], the authors propose a market equilibrium approach for fairly and efficiently allocating heterogeneous edge resources to multiple budget-constrained services. Cloudlet placement and workload allocation are jointly optimized in [12] to reduce the system response time, considering a fixed number of cloudlets. Farhadi *et al.* [13] propose a two-time-scale optimization model for the joint service placement and request scheduling problem under multi-dimensional resource and budget constraints.

In [14], the authors introduce a constant-factor approximation algorithm to determine an optimal service placement solution that maximizes the total user utility, considering the heterogeneity of user locations and edge resources. An IoT application provisioning problem is formulated in [15] to jointly optimize application placement and data routing to support all data streams while satisfying both bandwidth and delay requirements. Zhao *et al.* [16] present a ranking-based near optimal algorithm to efficiently deploy cloudlets among numerous APs in an IoT network. Lexicographic goal programming is used in [17] to address the user assignment problem for an SP whose goal is to minimize the number of required edge servers to run the service while maximizing the number of served users.

The edge service placement and resource management problem under uncertainty has attracted a lot of attention recently. Reference [18] presents a primal-dual online LP approach for optimal matching between multiple distributed ENs and multiple services arriving in an online fashion. In [19], the authors formulate the dynamic service placement problem as a contextual multi-armed bandit problem and propose a Thompson-sampling based online learning algorithm to help users select an EN for offloading, considering the tradeoff between latency and service migration cost. Badri *et al.* [20] cast an energy-aware multi-service placement problem under demand uncertainty as multi-stage stochastic problem, which aims to maximize the service quality under the energy budget constraint.

Distributionally robust optimization is utilized in [21] to tackle the edge service provisioning problem, with the goal of maximizing the expected revenue under the worst-case distribution of the uncertain demand. Li *et al.* [22] propose an approximation algorithm for the robust service function chain (SFC) placement and resource allocation problem, which aims to maximize the profit of a network operator considering demand uncertainty. In [2], we employ the KKT-based CCG approach to address the joint edge service placement and sizing problem under demand uncertainty.

A growing literature has focused on the service placement problem in EC from reliability and resiliency perspectives. Kherraf *et al.* [23] formulate an MIP for optimizing workload assignment to different ENs, considering a probabilistic reliability model for the ENs. Reference [24] studies a reliability-aware dynamic virtual network function (VNF) placement problem to minimize the placement cost while maximizing the number of admitted services. Chemodanov *et al.* [25] use chance-constrained programming to study the problem of reliable orchestration of latency-sensitive SFCs, considering probabilistic capacity constraints. Bian *et al.* [26] cast the distributed service chain composition problem with resource failures as a non-cooperative game and use weighted potential game to find an optimal Nash equilibrium to reduce request latency and network congestion.

In [27], the authors evaluate the failure resilience of a service deployed redundantly on the edge infrastructure by learning the spatio-temporal dependencies between edge server failures and exploiting the topological information to incorporate link failures. Then, they propose a dependency- and topology-aware failure resilience algorithm to minimize either redundancy cost or failure probability, while maintaining low network latency. Qu *et al.* [28] consider a

resilient edge service provisioning problem, which aims to maximize the expected utility from serving user requests at the edge in the presence of uncertain service failures. The authors formulate this as a static max-min RO problem and exploit the monotone submodular property to develop two approximation algorithms to solve the formulated problem. This is indeed a simplified model for our problem.

Different from the existing work, we propose a novel and rigorous two-stage robust model for joint edge service placement and workload allocation, considering both demand uncertainty and failure uncertainty. Furthermore, to the best of our knowledge, the proposed solution approaches are new in the cloud and edge computing literature.

6 CONCLUSION AND FUTURE WORK

In this paper, we proposed a two-stage robust optimization model for resilience-aware edge service placement and workload allocation. The proposed model can assist an SP to determine an optimal service placement and resource procurement solution in the first stage and optimize the workload allocation in the second stage, taking into account the uncertainties of both resource demand and EN failures. By implementing this model, the SP can not only drastically improve the user experience but also reduce its cost. To solve the underlying robust problem, we introduced three approaches, including two variants of the CCG algorithm and the ADR approach. Extensive numerical results confirm the efficacy of the proposed approaches. The conducted experiments also illustrate the advantages of the proposed two-stage adaptive robust model compared to the deterministic, stochastic, and heuristic methods.

There are several interesting directions for future work. First, we would like to integrate other types of failures, such as link failures and partial EN failures, into the proposed two-stage robust model. Second, we are interested in considering other uncertainty factors such as edge resource prices. Also, we would like to extend the model to consider VNF and multiple resource types, as well as multi-period workload allocation. Finally, we plan to modify the proposed model to study the robust edge network design problem from the perspective of an edge infrastructure provider.

REFERENCES

- [1] W. Shi, J. Cao, Q. Zhang, Y. Li, and L. Xu, "Edge computing: vision and challenges," *IEEE Internet Things J.*, vol. 3, no. 5, pp. 637–646, Oct. 2016.
- [2] D. T. Nguyen, H. T. Nguyen, N. Trieu, and V. K. Bhargava, "Two-stage robust edge service placement and sizing under demand uncertainty," *IEEE Internet Things J.*, to be published.
- [3] A. Ben-Tal, L. El Ghaoui, and A. Nemirovski, "Robust Optimization," Princeton, NJ, USA: Princeton Univ. Press, 2009.
- [4] B. Zeng and L. Zhao, "Solving two-stage robust optimization problems using a column-and-constraint generation method," *Oper. Res. L.*, pp. 457–461, vol. 41, no. 5, 2013.
- [5] D. Bertsimas and G. Vineet, "On the power and limitations of affine policies in two-stage adaptive optimization," *Math. Program.*, pp. 491–531, vol. 134, 2012.
- [6] A. Ben-Tal, A. Goryashko, and E. Guslitzer, "Adjustable robust solutions of uncertain linear programs," *Math. Program.*, vol. 99, pp. 351–376, 2004.
- [7] D. Kuhn, W. Wiesemann, and A. Georghiou, "Primal and dual linear decision rules in stochastic and robust optimization," *Math. Program.*, vol. 130, pp. 177–209, 2011.
- [8] J. Fortuny-Amat and B. McCarl, "A representation and economic interpretation of a two-level programming problem," *J. Oper. Res. Soc.*, vol. 32, no. 9, pp. 783–792, Sep. 1981.
- [9] D. Bertsimas and M. Sim, "The price of robustness," *J. Oper. Res.*, pp. 35–53, Feb. 2004.
- [10] D. T. Nguyen, L. B. Le, and V. Bhargava, "Price-based resource allocation for edge computing: a market equilibrium approach," *IEEE Trans. Cloud Comput.*, vol. 9, no. 1, pp. 302–317, Jan.–March 2021.
- [11] D. T. Nguyen, L. B. Le, and V. K. Bhargava, "A market-based framework for multi-resource allocation in fog computing," *IEEE/ACM Trans. Netw.*, vol. 27, no. 3, pp. 1151–1164, Jun. 2019.
- [12] M. Jia, J. Cao, and W. Liang, "Optimal cloudlet placement and user to cloudlet allocation in wireless metropolitan area networks," *IEEE Trans. Cloud Comput.*, vol. 5, no. 4, pp. 725–737, Oct.–Dec. 2017.
- [13] V. Farhadi, F. Mehmeti, T. He, T. L. Porta, H. Khamfroush, S. Wang, K.S. Chan, and K. Poularakis, "Service placement and request scheduling for data-intensive applications in edge clouds," *IEEE/ACM Trans. Netw.*, vol. 29, no. 2, pp. 779–792, Apr. 2021.
- [14] S. Pasteris, S. Wang, M. Herbster, and T. He, "Service placement with provable guarantees in heterogeneous edge computing systems," *Proc. IEEE INFOCOM*, Paris, France, Apr. 2019.
- [15] R. Yu, G. Xue, and X. Zhang, "Provisioning QoS-aware and robust applications in internet of things: a network perspective," *IEEE/ACM Trans. Netw.*, vol. 27, no. 5, pp. 1931–1944, Oct. 2019.
- [16] L. Zhao, W. Sun, Y. Shi, and J. Liu, "Optimal placement of cloudlets for access delay minimization in SDN-based internet of things networks," *IEEE Internet Things J.*, vol. 5, no. 2, pp. 1334–1344, April 2018.
- [17] P. Lai et al., "Cost-effective app user allocation in an edge computing environment," *IEEE Trans. Cloud Comput.*, to be published.
- [18] D. T. Nguyen, L. B. Le, and V. K. Bhargava, "Edge computing resource procurement: an online optimization approach," *Proc. IEEE WF-IoT*, pp. 807–812, Singapore, 2018.
- [19] T. Ouyang, R. Li, X. Chen, Z. Zhou and X. Tang, "Adaptive user-managed service placement for mobile edge computing: an online learning approach," in *Proc. IEEE INFOCOM*, pp. 1468–1476, Paris, France, 2019.
- [20] H. Badri, T. Bahreini, D. Grosu, and K. Yang, "Energy-aware application placement in mobile edge computing: a stochastic optimization approach," *IEEE Trans. Parallel Distrib. Syst.*, vol. 31, no. 4, pp. 909–922, Apr. 2020.
- [21] L. Li, D. Shi, R. Hou, X. Li, J. Wang, H. Li, and M. Pan, "Data-driven optimization for cooperative edge service provisioning with demand uncertainty," in *IEEE Internet Things J.*, vol. 8, no. 6, pp. 4317–4328, Mar. 2021.
- [22] J. Li, W. Liang, and Y. Ma, "Robust service provisioning with service function chain requirements in mobile edge computing," *IEEE Trans. Netw. Serv. Manag.*, vol. 18, no. 2, pp. 2138–2153, Jun. 2021.
- [23] N. Kherraf, S. Sharafeddine, C. Assi, and A. Ghayeb, "Latency and reliability-aware workload assignment in IoT networks with mobile edge clouds," *IEEE Trans. Netw. Ser. Manag.*, vol. 16, no. 4, pp. 1435–1449, Dec. 2019.
- [24] M. Karimzadeh-Farshbafan, V. Shah-Mansouri, and D. Niyato, "A dynamic reliability-aware service placement for network function virtualization (NFV)," *IEEE J. Sel. Areas Commun.*, vol. 38, no. 2, pp. 318–333, Feb. 2020.
- [25] D. Chemodanov, P. Callyam, F. Esposito, R. McGarvey, K. Palaniappan and A. Pescapé, "A near optimal reliable orchestration approach for geo-distributed latency-sensitive SFCs," *IEEE Trans. Netw. Sci. Eng.*, vol. 7, no. 4, pp. 2730–2745, Oct.–Dec. 2020.
- [26] S. Bian, X. Huang, Z. Shao, X. Gao, and Y. Yang, "Service chain composition with resource failures in NFV systems: a game-theoretic perspective," *IEEE Trans. Netw. Serv. Manag.*, vol. 18, no. 1, pp. 224–239, Mar. 2021.
- [27] A. Aral and I. Brandić, "Learning spatio-temporal failure dependencies for resilient edge computing services," *IEEE Trans. Parallel Distrib. Syst.*, vol. 32, no. 7, pp. 1578–1590, Jul. 2021.
- [28] Y. Qu et al., "Resilient service provisioning for edge computing," *IEEE Internet Things J.*, to be published.
- [29] Y. Mao, C. You, J. Zhang, K. Huang, and K. B. Letaief, "A survey on mobile edge computing: the communication perspective," *IEEE Commun. Surv. Tut.*, vol. 19, no. 4, pp. 2322–2358, Fourthquarter 2017.
- [30] [Access June 2021] <https://aws.amazon.com/ec2/pricing/>
- [31] [Access June 2021] <http://gwa.ewi.tudelft.nl/datasets/>

7 APPENDIX

7.1 Convergence of Algorithm 1

Because Ξ^e has a finite number of K elements, to prove the *Proposition 3.1*, we only need to show that before convergence, the subproblem always outputs a distinct extreme point at every iteration. In other words, if any extreme point (z^*, λ^*) is repeated at two iterations, then $LB = UB$, which means convergence. We can show it as follows.

Assume (x^*, y^*, t^*, η^*) is an optimal solution to the **MP** and $(z^*, \lambda^*, w^*, q^*)$ is an optimal solution to the subproblem in iteration k . Also, the extreme point (z^*, λ^*) has appeared in a previous iteration. From the definition of the UB in (19), we have:

$$UB \leq (1 - \rho) \left\{ \sum_j p_j y_j^* + \sum_j h_j t_j^* + \beta \sum_{i,j} d_{i,j} x_{i,j}^* \right\} + \rho \left\{ \sum_i P_i q_i^* + \beta \sum_{i,j} d_{i,j} w_{i,j}^* \right\}. \quad (30)$$

Since (z^*, λ^*) appeared in a previous iteration, the cuts related to (z^*, λ^*) to be added to the **MP** at iteration $k + 1$ has already been added previously to the **MP**. Thus, the **MP** in iteration $k + 1$ is identical to **MP** in iteration k . Hence, (x^*, y^*, t^*, η^*) is also the optimal solution to the **MP** in iteration $k + 1$. Note that we have:

$$LB \geq (1 - \rho) \left\{ \sum_j h_j t_j^* + \sum_j p_j y_j^* + \beta \sum_{i,j} d_{i,j} x_{i,j}^* \right\} + \rho \eta^* \quad (31)$$

On the other hands, since $(z^*, \lambda^*, w^*, q^*)$ is an optimal solution to the subproblem in iteration k , from (18), obviously we have

$$\sum_j P_i q_i^* + \beta \sum_{i,j} d_{i,j} w_{i,j}^* \leq \sum_j P_i q_i + \beta \sum_{i,j} d_{i,j} w_{i,j}, \quad (32)$$

for **every** (w, q) that satisfies constraints (18b)-(18f) given $z = z^*$ and $\lambda = \lambda^*$. Since the extreme point (z^*, λ^*) has already been identified and related constraints are added to the **MP** before iteration k , there exists $j \leq k$ where (w^l, q^l) needs to satisfy constraints (18b)-(18f) given $z = z^*$ and $\lambda = \lambda^*$. From (15b) and (32), at iteration k we have:

$$\sum_j P_i q_i^* + \beta \sum_{i,j} d_{i,j} w_{i,j}^* \leq \sum_j P_i q_i^l + \beta \sum_{i,j} d_{i,j} w_{i,j}^l \leq \eta^*. \quad (33)$$

From (30), (31), and (33), we have: $LB \geq UB$, which implies $LB = UB$ because LB cannot exceed UB. Thus, any repeated extreme point $\xi^* = (z^*, \lambda^*)$ implies convergence. Since Ξ^e is a finite set with K elements, the proposed algorithm is guaranteed to converge in $O(K)$ iterations.

7.2 KKT-based subproblem reformulation

The Lagrangian function of the inner minimization problem in the subproblem is:

$$\begin{aligned} \mathcal{L}(w_{i,j}, q_i, s_i, u_j, \gamma_{i,j}^1, \gamma_i^2) = & \rho \left\{ \sum_i P_i q_i + \beta \sum_{i,j} d_{i,j} w_{i,j} \right\} \\ & - \sum_i \gamma_i^2 q_i - \sum_{i,j} \gamma_{i,j}^1 w_{i,j} + \sum_j u_j^1 \left(\sum_i w_{i,j} - (1 - z_j) C_j \hat{t}_j \right) \\ & \sum_j u_j^2 \left(\sum_i w_{i,j} - \hat{y}_j \right) + \sum_i s_i (\bar{\lambda}_i + g_i \tilde{\lambda}_i - q_i - \sum_j w_{i,j}) \\ & + \sum_{i,j} \pi_{i,j} (w_{i,j} - a_{i,j} C_j) \end{aligned}$$

The KKT conditions are:

$$\frac{\partial \mathcal{L}}{\partial w_{i,j}} = \beta \rho d_{i,j} + u_j + \pi_{i,j} - s_i = \gamma_{i,j}^1 \geq 0, \forall i, j \quad (34a)$$

$$\frac{\partial \mathcal{L}}{\partial q_i} = \rho P_i - s_i = \gamma_i^2 \geq 0, \forall i \quad (34b)$$

$$\sum_j w_{i,j} + q_i \geq \lambda_i, \forall i \quad (34c)$$

$$\sum_i w_{i,j} \leq C_j \hat{t}_j (1 - z_j); \quad \sum_i w_{i,j} \leq \hat{y}_j, \forall j \quad (34d)$$

$$0 \leq w_{i,j} \leq a_{i,j} C_j, \forall i, j; \quad q_i \geq 0, \forall i \quad (34e)$$

$$\gamma_{i,j}^1, \pi_{i,j} \geq 0, \forall i, j; \quad \gamma_i^2, s_i \geq 0, \forall i; \quad u_j^1, u_j^2 \geq 0, \forall j \quad (34f)$$

$$(\lambda_i - \sum_j w_{i,j} - q_i) s_i = 0, \forall i \quad (34g)$$

$$\left(\sum_i w_{i,j} - (1 - z_j) C_j \hat{t}_j \right) u_j^1 = 0, \forall j \quad (34h)$$

$$\left(\sum_i w_{i,j} - \hat{y}_j \right) u_j^2 = 0, \forall j \quad (34i)$$

$$(w_{i,j} - a_{i,j} C_j) \pi_{i,j} = 0, \forall i, j \quad (34j)$$

$$w_{i,j} \gamma_{i,j}^1 = 0, \forall i, j \quad q_i \gamma_i^2 = 0, \forall i \quad (34k)$$

where (34a) and (34b) are the stationary conditions, (34c) - (34e) are the primal feasibility conditions, (34f) is dual feasibility condition, and (34g) - (34k) are the complementary slackness conditions. We can then re-write the subproblem with complementary constraints:

$$\max_{(\lambda, z) \in \Xi, w, q} \rho \left\{ \sum_i P_i q_i + \beta \sum_{i,j} d_{i,j} w_{i,j} \right\} \quad (35a)$$

$$\text{s.t. } 0 \leq \rho P_i d_{i,j} + u_j - s_i \perp w_{i,j}, \forall i, j \quad (35b)$$

$$0 \leq \rho P_i - s_i \perp q_i \geq 0, \forall i \quad (35c)$$

$$0 \leq C_j \hat{t}_j (1 - z_j) - \sum_i w_{i,j} \perp u_j^1 \geq 0, \forall j \quad (35d)$$

$$0 \leq \hat{y}_j - \sum_i w_{i,j} \perp u_j^2 \geq 0, \forall j \quad (35e)$$

$$0 \leq \sum_j w_{i,j} + q_i - \bar{\lambda}_i - g_i \tilde{\lambda}_i \perp s_i \geq 0, \forall i \quad (35f)$$

$$0 \leq a_{i,j} C_j - w_{i,j} \perp \pi_{i,j} \geq 0, \forall i, j \quad (35g)$$

$$\sum_i g_i \leq \Gamma; \quad g_i \in [0, 1], \forall i; \quad \sum_j z_j \leq K; \quad z_j \in \{0, 1\}, \forall j, \quad (35h)$$

where (35h) is the constraint in uncertainty set Ξ . Note that a complimentary constraint $0 \leq x \perp \gamma \geq 0$ implies a set of constraints including $(x \geq 0, \gamma \geq 0, x\gamma = 0)$. Notice

that there exists an bilinear term between primal variable x and its dual variable γ . Fortunately, this non-linear complimentary constraint can be transformed into exact linear constraints by using Fortuny-Amat transformation [8]. Let M be the sufficient large number and v be the binary variable. The equivalent transformation of complementary constraint is shown as follows:

$$0 \leq x \leq vM \quad (36a)$$

$$0 \leq \gamma \leq (1-v)M \quad (36b)$$

By applying this transformation for all complimentary constraints (34g) to (34k), we can get exact form of problem shown in (20).

7.3 ADR Reformulation

To transform the ADR model (27) into an MILP, we need to reformulate each robust constraint from (27c) to (27i) as an equivalent set of linear equations. First, consider constraint (27c). It is easy to see that (27c) is equivalent to:

$$\begin{aligned} \phi \geq & \max_{g,z} \sum_{i \in I} P_i \left[\sum_{e \in I} E_i^e (\bar{\lambda}_e + g_e \tilde{\lambda}_e) + \sum_{l \in J} F_i^l z_l + G_i \right] \\ & + \beta \sum_{i \in I} \sum_{j \in J} d_{i,j} \left[\sum_{e \in I} A_{i,j}^e (\bar{\lambda}_e + g_e \tilde{\lambda}_e) + \sum_{l \in J} B_{i,j}^l z_l + D_{i,j} \right] \end{aligned} \quad (37a)$$

$$\text{s.t.} \quad \sum_e g_e \leq \Gamma, \quad (\mu^0) \quad (37b)$$

$$0 \leq g_e \leq 1, \quad \forall e \quad (\eta_e^0) \quad (37c)$$

$$\sum_j z_l \leq k, \quad (v^0) \quad (37d)$$

$$0 \leq z_l \leq 1, \quad \forall l, \quad (\sigma_l^0) \quad (37e)$$

where μ^0 , η_e^0 , v_0 , and σ_l^0 are dual variables for constraints from (37b) to (37e), respectively. Be rearranging the terms in problem (37), we can rewrite problem (37) as follows:

$$\begin{aligned} \phi \geq & \sum_{i \in I} \sum_{e \in I} P_i E_i^e \bar{\lambda}_e + \sum_{i \in I} P_i G_i + \beta \sum_{i \in I} \sum_{j \in J} \sum_{e \in I} d_{i,j} A_{i,j}^e \bar{\lambda}_e \\ & + \beta \sum_{i \in I} \sum_{j \in J} d_{i,j} D_{i,j} + \max_{g,z} \left\{ \sum_{i \in I} \sum_{l \in J} P_i F_i^l z_l \right. \\ & + \sum_{i \in I} \sum_{e \in I} P_i E_i^e g_e \tilde{\lambda}_e + \beta \sum_{i \in I} \sum_{j \in J} \sum_{l \in J} d_{i,j} B_{i,j}^l z_l \\ & \left. + \beta \sum_{i \in I} \sum_{j \in J} \sum_{e \in I} d_{i,j} A_{i,j}^e g_e \tilde{\lambda}_e \right\} \end{aligned} \quad (38a)$$

$$\text{s.t.} \quad \sum_e g_e \leq \Gamma, \quad (\mu^0) \quad (38b)$$

$$0 \leq g_e \leq 1, \quad \forall e \quad (\eta_e^0) \quad (38c)$$

$$\sum_j z_l \leq k, \quad (v^0) \quad (38d)$$

$$0 \leq z_l \leq 1, \quad \forall l, \quad (\sigma_l^0) \quad (38e)$$

By LP theory, the dual of the maximization problem on the right hand side of (38) is the following linear minimiza-

tion problem. Thus, problem (38) (i.e., the robust constraint (27c)) is equivalent to the following set of linear equations:

$$\begin{aligned} \phi - & \sum_{i \in I} \sum_{e \in I} P_i E_i^e \bar{\lambda}_e - \sum_{i \in I} P_i G_i - \beta \sum_{i \in I} \sum_{j \in J} \sum_{e \in I} d_{i,j} A_{i,j}^e \bar{\lambda}_e \\ & - \beta \sum_{i \in I} \sum_{j \in J} d_{i,j} D_{i,j} - kv^0 - \Gamma \mu^0 - \sum_{e \in I} \eta_e^0 - \sum_{l \in J} \sigma_l^0 \geq 0 \end{aligned} \quad (39a)$$

$$\eta_e^0 + \mu^0 \geq \beta \sum_{i \in I} \sum_{j \in J} d_{i,j} A_{i,j}^e \tilde{\lambda}_e + \sum_{i \in I} P_i E_i^e \tilde{\lambda}_e, \quad \forall e \quad (39b)$$

$$\sigma_l^0 + v^0 \geq \beta \sum_{i \in I} \sum_{j \in J} d_{i,j} B_{i,j}^l + \sum_{i \in I} P_i F_i^l, \quad \forall l \quad (39c)$$

$$\eta_e^0, v^0, \mu^0 \geq 0; \quad \sigma_l^0 \geq 0, \quad \forall l. \quad (39d)$$

By following similar procedure, we can reformulate individual robust constraints from (27d) to (27i) into equivalent sets of linear equations. For the sake of brevity, we will present the final set of equations for each constraint only. Specifically, (27d) is equivalent to:

$$\begin{aligned} \sum_{i \in I} \sum_{e \in I} A_{i,j}^e \bar{\lambda}_e + \sum_{i \in I} D_{i,j} - C_j \hat{t}_j + \sum_{e \in I} \eta_{e,j}^1 + \Gamma \mu_j^1 \\ + \sum_{l \in J} \sigma_{l,j}^1 + kv_j^1 \leq 0, \quad \forall j \end{aligned} \quad (40a)$$

$$\eta_{e,j}^1 + \mu_j^1 \geq \sum_{i \in I} A_{i,j}^e \tilde{\lambda}_e, \quad \forall e, j \quad (40b)$$

$$\sigma_{l,j}^1 + v_j^1 \geq \sum_{i \in I} B_{i,j}^l, \quad \forall l, l \neq j \quad (40c)$$

$$\sigma_{l,j}^1 + v_j^1 \geq \sum_{i \in I} B_{i,j}^l + C_j \hat{t}_j; \quad \forall j, l = j \quad (40d)$$

$$\eta_{e,j}^1 \geq 0, \quad \forall e, j; \quad v_j^1, \mu_j^1 \geq 0, \quad \forall j; \quad \sigma_{l,j}^1 \geq 0, \quad \forall l, j. \quad (40e)$$

The equivalent reformulation of constraint (27e) is:

$$\begin{aligned} \sum_{i \in I} \sum_{e \in I} A_{i,j}^e \bar{\lambda}_e + \sum_{i \in I} D_{i,j} - y_j + \sum_{e \in I} \eta_{e,j}^1 + \Gamma \mu_j^1 \\ + \sum_{l \in J} \sigma_{l,j}^1 + kv_j^1 \leq 0, \quad \forall j \end{aligned} \quad (41a)$$

$$\eta_{e,j}^2 + \mu_j^2 \geq \sum_{i \in I} A_{i,j}^e \tilde{\lambda}_e, \quad \forall e, j \quad (41b)$$

$$\sigma_{l,j}^2 + v_j^2 \geq \sum_{i \in I} B_{i,j}^l, \quad \forall l \quad (41c)$$

$$\eta_{e,j}^2 \geq 0, \quad \forall e, j; \quad v_j^2, \mu_j^2 \geq 0, \quad \forall j; \quad \sigma_{l,j}^2 \geq 0, \quad \forall l, j. \quad (41d)$$

Similarly, constraint (27f) is equivalent to:

$$\begin{aligned} \sum_{j \in J} \sum_{e \in I} A_{i,j}^e \bar{\lambda}_e + \sum_{e \in I} E_i^e \bar{\lambda}_e + \sum_{j \in J} D_{i,j} + G_i - \bar{\lambda}_i \\ - \sum_{e \in I} \eta_{i,e}^3 - \Gamma \mu_i^3 - \sum_{l \in J} \sigma_{i,l}^3 - kv_i^3 \geq 0, \quad \forall i \end{aligned} \quad (42a)$$

$$\eta_{i,e}^3 + \mu_i^3 \geq - \sum_{j \in J} A_{i,j}^e \tilde{\lambda}_e - E_{i,e} \tilde{\lambda}_e, \quad \forall i, e \quad (42b)$$

$$\eta_{i,e}^3 + \mu_i^3 \geq - \sum_{j \in J} A_{i,j}^e \tilde{\lambda}_e - E_{i,e} \tilde{\lambda}_e + \tilde{\lambda}_i, \quad \forall i, e = i \quad (42c)$$

$$\sigma_{i,l}^3 + v_i^3 \geq - \sum_{j \in J} B_{i,j}^l - F_i^l, \quad \forall i, l \quad (42d)$$

$$\eta_{i,e}^3 \geq 0, \quad \forall i, e; \quad v_i^3, \mu_i^3 \geq 0, \quad \forall i; \quad \sigma_{i,l}^3 \geq 0, \quad \forall i, l. \quad (42e)$$

Constraint (27g) is equivalent to:

$$\sum_{e \in I} E_i^e \bar{\lambda}_e + G_i - \sum_{e \in I} \eta_{i,e}^3 - \Gamma \mu_i^4 - \sum_{l \in J} \sigma_{i,l}^4 - kv_i^4 \geq 0, \forall i \quad (43a)$$

$$-\eta_{i,e}^4 - \mu_i^4 \leq E_i^e \bar{\lambda}_e, \forall i, e \quad (43b)$$

$$-\sigma_{i,l}^4 - v_i^4 \leq F_i^l, \forall i, l \quad (43c)$$

$$\eta_{i,e}^4 \geq 0, \forall i, e; v_i^4, \mu_i^4 \geq 0, \forall i, j; \sigma_{i,l}^4 \geq 0, \forall i, l. \quad (43d)$$

Constraint (27h) is equivalent to:

$$\sum_e A_{i,j}^e \bar{\lambda}_e + D_{i,j} - \sum_e \eta_{i,j,e}^5 - \Gamma \mu_{i,j}^5 - \sum_l \sigma_{i,j,l}^5 - kv_{i,j}^5 \geq 0, \forall i, j \quad (44a)$$

$$-\eta_{i,j,e}^5 - \mu_{i,j}^5 \leq A_{i,j}^e \bar{\lambda}_e, \forall i, j, e \quad (44b)$$

$$-\sigma_{i,j,l}^5 - v_{i,j}^5 \leq B_{i,j}^l, \forall i, j, l \quad (44c)$$

$$\eta_{i,j,e}^5 \geq 0, \forall i, j, e; v_{i,j}^5, \mu_{i,j}^5 \geq 0, \forall i, j; \sigma_{i,j,l}^5 \geq 0, \forall i, j, l. \quad (44d)$$

Finally, constraint (27i) is equivalent to:

$$\sum_e A_{i,j}^e \bar{\lambda}_e + D_{i,j} - \sum_e \eta_{i,j,e}^6 - \Gamma \mu_{i,j}^6 - \sum_l \sigma_{i,j,l}^6 - kv_{i,j}^6 \leq a_{i,j} C_j, \forall i, j \quad (45a)$$

$$-\eta_{i,j,e}^6 - \mu_{i,j}^6 \leq A_{i,j}^e \bar{\lambda}_e, \forall i, j, e \quad (45b)$$

$$-\sigma_{i,j,l}^6 - v_{i,j}^6 \leq B_{i,j}^l, \forall i, j, l \quad (45c)$$

$$\eta_{i,j,e}^6 \geq 0, \forall i, j, e; v_{i,j}^6, \mu_{i,j}^6 \geq 0, \forall i, j; \sigma_{i,j,l}^6 \geq 0, \forall i, j, l. \quad (45d)$$

By replacing the sets of constraints from (39) to (45) into the ADR model (27), we obtain the MILP as shown in (28).

7.4 Deterministic Formulation

The deterministic formulation of the service placement and sizing problem is the following MILP problem:

$$\min_{x,t,w,q} \sum_j p_j y_j + \sum_j h_j t_j + \sum_i P_i q_i + \beta \sum_{i,j} d_{i,j} w_{i,j} \quad (46a)$$

$$\text{s.t.} \sum_j p_j y_j + f_j(1-t_0)t_j \leq B \quad (46a)$$

$$0 \leq y_j \leq C_j t_j, \forall j \quad (46b)$$

$$\sum_i w_{i,j} \leq y_j t_j, \forall j \quad (46c)$$

$$\sum_j w_{i,j} + q_i \geq \lambda_i^f, \forall i \quad (46d)$$

$$0 \leq w_{i,j} \leq a_{i,j} C_j, \forall i, j \quad (46e)$$

$$t_j \in \{0, 1\}, \forall j; y_j \in \mathbb{Z}, \forall j; q_i \geq 0, \forall i. \quad (46f)$$

In the deterministic algorithm, the SP first solves this deterministic problem, using the forecast demand λ to obtain the optimal service placement and resource procurement solution (t^*, y^*) . In the actual operation stage, after observing the actual realization of the demand and EN failures, given the (t^*, y^*) as the input, the SP will solve problem (12) to find the optimal workload allocation decision (w, q) .

7.5 The Two-stage Stochastic Programming Model

Instead of optimizing the workload allocation in the worst-case uncertainty realization in the second stage as in the ARO model (\mathcal{P}_1), in the stochastic model, the SP aims to optimize the expected cost in the second stage. Let $\xi = \{\xi^1, \dots, \xi^n, \dots, \xi^N\}$ be the set of N scenarios representing the uncertainties of the demand and EN failures, n is the scenario index and $\xi^n = (\lambda^n, z^n)$. Also, denote by π^n the probability scenario n . The two-stage stochastic edge service placement and workload allocation model is:

$$\min_{x,y,t,w,q} (1-\rho) \left\{ \sum_j p_j y_j + \sum_j f_j(1-t_0)t_j + \beta \sum_{i,j} d_{i,j} x_{i,j} \right\} + \rho \sum_{n=1}^N \pi_n \left\{ \beta \sum_i \sum_j d_{i,j}^n w_{i,j}^n + \sum_i P_i^n q_i^n \right\} \quad (47a)$$

$$\text{s.t.} \sum_j x_{i,j} \geq \lambda_i^f, \forall i \quad (47b)$$

$$\sum_i x_{i,j} \leq \sum_j y_j \leq C_j t_j, \forall j \quad (47c)$$

$$\sum_j p_j y_j + \sum_j h_j t_j \leq B, \quad (47d)$$

$$0 \leq x_{i,j} \leq a_{i,j} C_j, \forall i, j \quad (47e)$$

$$\sum_i w_{i,j}^n \leq y_j t_j (1-z_j^n), \forall j, n \quad (47f)$$

$$q_i^n + \sum_j w_{i,j}^n \geq \lambda_i^n, \forall i, n \quad (47g)$$

$$t_j \in \{0, 1\}, \forall j; y_j \in \mathbb{Z}, \forall j \quad (47h)$$

$$0 \leq w_{i,j}^n \leq a_{i,j} C_j, \forall i, j, n; q_i^n \geq 0, \forall i, n, \quad (47i)$$

where (w^n, q^n) expresses the second-stage decision corresponding to scenario n .